# Fisher information and temporal correlations for spiking neurons with stochastic dynamics

Jan Karbowski
*Center for Biodynamics, Department of Mathematics, Boston University, Boston, Massachusetts 02215*
*and Center for Theoretical Physics, Polish Academy of Sciences, 02-668 Warsaw, Poland*
(Received 25 June 1999)

Population coding accuracy can be studied using Fisher information. Here the Fisher information and correlation functions are determined analytically for a network of coupled spiking neurons with a more general than Poisson stochastic dynamics. It is shown that stimulus-driven temporal correlations between neurons always increase the Fisher information, whereas stimulus-independent correlations need not do so. Additionally, we find that for subthreshold stimuli there is some nonzero level of noise for which network coding is optimal. We also find that the Fisher information is larger for purely excitatory than for purely inhibitory networks, but only in a limited range of values of synaptic coupling strengths. In most cases the dependence of the Fisher information on time is linear, except for excitatory networks with strong synaptic couplings and for strong stimuli. In the latter case this dependence shows two distinct regimes: fast and slow. For excitatory networks short-term synaptic depression can improve the coding accuracy significantly, whereas short-term facilitation can lower the coding accuracy. For inhibitory networks, coding accuracy is insensitive to short-term synaptic dynamics.

PACS number(s): 87.18.Sn, 84.35.+i, 87.19.Dd, 87.19.La

## I. INTRODUCTION

Information-theoretic approaches in computational neuroscience have become more popular recently [1–8]. One of the reasons for this is that information theory can provide not only qualitative but also quantitative descriptions of neural encoding. Neural encoding can be studied by measuring neural responses in sensory systems as a function of an external stimulus. Based on those responses one can estimate what was the value of encoded variable [2,10–15]; for a review, see Ref. [16].

In the presence of noise in a neural network it is not trivial to decode accurately some variable $x$ from the activity pattern $\{s\}$ of the population of neurons. On a trial to trial basis there will be a discrepancy between a true value $x$ of a stimulus and its estimated value $x_{est}(\{s\})$. Since human and animal performances in sensory and motor tasks are often very reliable, one can anticipate that the nervous system usually tries to minimize that discrepancy.

In information theory there are useful quantities for investigating the accuracy of population coding. One of them is the standard mutual information between the input and output of the system; a second, less often used quantity, is called Fisher information [17]. Both of these quantities measure the degree of correlation between an input and an output. The Fisher information measures information about a given value of the stimulus, whereas the mutual information measures information about a distribution of possible values. In this work we consider the Fisher information.

The Fisher information $I_F(x)$ is a measure of the encoding accuracy of some quantity $x$, because it is related to the lower bound of the variance of the estimator $x_{est}$, which is equal to $\langle (x_{est}-x)^2 \rangle$, by an expression

$$\langle (x_{est}-x)^2 \rangle \geqslant \frac{1}{I_F(x)}, \tag{1}$$

where $\langle x^n_{est} \rangle = \Sigma_{\{s\}} P[\{s\};x] x^n_{est}(\{s\})$; i.e. symbol $\langle x^n_{est} \rangle$ denotes an averaging of the estimator $x^n_{est}(\{s\})$ over the activity of neurons $\{s\}$ represented by some distribution function $P[\{s\};x]$, given a stimulus value $x$ (in this paper $x$ is a scalar variable). The right hand side of the above inequality, which is valid for all unbiased estimation methods, i.e., when $\langle x_{est} \rangle = x$ [17], is known as the Cramer-Rao bound. In general, it is not obvious that this lower bound can be reached by an arbitrarily chosen decoding scheme. Nevertheless, there exist some examples where this is possible [15,18]. From Eq. (1), we see that a population of neurons can optimally (in principle) extract the value of a stimulus by maximizing $I_F$.

Recently the question of the relationship between population coding accuracy and correlations among neurons attracted much attention [19–25]. In cases where one considers the average activity of neurons, neglecting the temporal pattern of spikes, the answer to this question turned out to be inconclusive both experimentally [19,20,24] and theoretically [6,26]. That is, there examples were found of increased and decreased accuracy of population coding by correlations. However, when one considers the fine temporal structure of spiking neurons, there are experimental indications that simultaneous firing, i.e., precise temporal correlations, may actually help in coding [21–23,25].

This paper studies the relation between temporal correlations among neurons and the accuracy of population coding using the concepts of correlation functions and Fisher information. We derive explicit expressions for those quantities in the sparsely connected neural network. Additionally, we determine which of the factors—noise, the type of synaptic coupling, short-term synaptic dynamics, and the size of neuronal population—increase the Fisher information (hence improve the coding accuracy), and under what circumstances. The Fisher information was studied before in the context of the accuracy of population coding [4–6,8,9]. Those papers either did not consider correlations between neurons [4,5] or take into account correlations, but neglect the fine temporal structure of neural activity [6,8,9]. In contrast to those papers, we investigate a stochastic network

 

model of spiking coupled neurons with a more general than Poisson dynamics. Specifically, we do not assume any particular type of correlation for noise between neurons. Instead, we assume that the network dynamics is governed by a certain stochastic process caused by some intrinsic noise in the network, as well as by an external stimulus. The resulting correlations between neurons consist of stimulus-driven and stimulus-independent correlations. The latter are the result of intrinsic ''noisy'' dynamics mediated by synaptic coupling. In the approaches of Abbott and Dayan [6] and Zhang and Sejnowski [8], one cannot distinguish between these two types of correlations. The network approach taken in this paper provides a natural distinction between them.

The main result of this paper is to show that there is a monotonic relation between stimulus-driven temporal correlations and the accuracy of population coding. This means that the stronger these correlations, the larger the Fisher information and more accurate the coding. However, there is no systematic dependence between stimulus-independent temporal correlations and the Fisher information if the driving input is subthreshold. For suprathreshold inputs, these correlations always lower the coding accuracy. The finding that stimulus-driven temporal correlations between neurons improve the accuracy of coding is consistent with experimental results of Dan *et al.* [25].

Additionally, it is shown that there is some nonzero level of noise for subthreshold stimuli for which the Fisher information is optimal. This behavior resembles the phenomenon of the ''stochastic resonance'' found in some parts of the nervous system [27–30]; for a review, see Ref. [31].

Another finding is that there is a relationship between the type of synaptic coupling and the accuracy of the coding. The Fisher information has a maximum for positive values of synaptic couplings, suggesting that excitatory networks perform better than inhibitory networks. However, inhibitory networks are more broadly tuned, which may, in certain cases, be more advantageous. We made computations for networks with homogeneous couplings between neurons either purely excitatory or purely inhibitory. This greatly simplifies the analysis, which is already complicated.

The dependence of the Fisher information on the time course is linear for inhibitory networks regardless of the strength of synapses and stimulus. Excitatory networks show a different behavior. For weak coupling and weak stimuli, the dependence is linear, whereas for strong coupling with strong stimuli there are two distinct regimes. The initial regime exhibits very fast growth, while a subsequent regime shows slower growth. Possible functional consequences of this behavior are discussed in Sec. V.

The impact of short-term synaptic dynamics on the Fisher information is also studied. It is found that synaptic depression can improve the coding accuracy by an order of magnitude for a network of purely excitatory cells with sufficiently strong coupling and for strong stimuli. On the other hand, synaptic facilitation can decrease the coding accuracy for a population of excitatory cells, but not in such a dramatic way. Short-term synaptic dynamics does not have any noticeable influence on coding for purely inhibitory networks. We also confirm previous findings that the Fisher information grows linearly with the size of the network [6], and additionally, that it is optimal for narrowly tuned driving inputs [8], regardless of the fact whether neurons are correlated or not.

The basic ideas and results are provided in the main text of the paper. Details about particular derivations are presented in the Appendixes.

## II. NETWORK DYNAMICS

In the presence of noise in a network, the output of a given neuron is represented by the probability that the neuron will fire. This probability, in general, depends on the state of the present and past activities of all neurons in the network; therefore, it is a conditional probability. We model the probability that neuron $\alpha$ is in state $s_\alpha(k+1)$ at time step $k+1$ by a discrete-time model with a length of a time step $\tau$ as

$$P[s_\alpha(k+1)|\{s(1)\},\{s(2)\},\ldots,\{s(k)\};x] = \frac{1}{2}\left(1+[2s_\alpha(k+1)-1]\tanh\left[\frac{R_\alpha(k)}{\eta}\right]\right). \quad (2)$$

For our purposes, it is sufficient to assume that the activity of neurons in the network can be adequately described by a two-state neuron model, i.e., $s_\alpha(k)=1$ if neuron $\alpha$ fires at time step $k$, and $s_\alpha(k)=0$ if it does not [32,33]. Symbol $\{s(k)\}$ represents the activity of all neurons in the network at time step $k$. The time unit $\tau$ can be of the order of an effective membrane time constant or refractory period. The parameter $\eta$ is a measure of noise in the network. For $\eta=0$ the network is noiseless, whereas for $\eta\mapsto\infty$ the noise is maximal. In the latter limit the probability of firing [Eq. (2)], at any given time step $k$ is always equal to 1/2. The choice for the probability given by Eq. (2) is motivated by the fact that it has a sigmoidal shape as a function of $R_\alpha(k)$. This type of stochastic dynamics was pioneered in condensed matter physics in studying Ising-type models with thermal noise (for example, cf. Ref. [34]). A later, similar dynamics was used by others in other contexts, namely, to study temporal associations [35] and correlations in the Markov-type neural model [36].

The function $R_\alpha(k)$ in Eq. (2) contains the entire information about the activity of all other neurons at earlier times up to $k$ step. We represent $R_\alpha(k)$ in a standard way:

$$R_\alpha(k)=\sum_{\beta\neq\alpha}\tilde{J}_{\alpha\beta}(k)s_\beta(k)+c_\alpha(x)-\theta. \quad (3)$$

Here $c_\alpha(x)$ is a time-independent driving input or a drive to the neuron $\alpha$ caused by an external stimulus $x$; $\theta$ is a threshold for firing (when noise is absent), identical for all neurons; and $\tilde{J}_{\alpha\beta}(k)$ is a time-dependent synaptic coupling from the presynaptic neuron $\beta$ to the postsynaptic neuron $\alpha$. We choose this coupling to be time dependent because we want to include the effect of short-term synaptic plasticity [37,38]. The synaptic coupling is modeled in the form

$$\tilde{J}_{\alpha\beta}(k)=[1-as_\beta(k-1)]J_{\alpha\beta}. \quad (4)$$

This form mimics short-term synaptic dynamics effects through the presence of a parameter $a(|a|<1)$. Negative values of $a$ correspond to synaptic facilitation, while its positive values correspond to synaptic depression. Equation (4) shows that when the presynaptic neuron $\beta$ fires at time step $k-1$, the synaptic strength from neuron $\beta$ to neuron $\alpha$ at time step $k$ will be reduced (or amplified if $a<0$) by a factor $(1-a)$. Our model of the network dynamics is not Markovian when the short-term synaptic dynamics is taken into account. We recover Markovian dynamics in the limit $a\mapsto 0$.

In Eq. (4), time-independent coupling $J_{\alpha\beta}$ is represented by $J_{\alpha\beta}=J\Sigma_{\gamma=1}^{N}\delta_{\alpha,\beta+\gamma}$, which means that we assume that each presynaptic neuron $\beta$ is connected to $N$ postsynaptic neurons $\beta+1,\ldots,\beta+N$, with the same strength $J$, where $N$ is a number of synaptic connections. Additionally, we assume that the number of these connections for a given neuron is much smaller than the number of neurons $N_0$ in the network, i.e., $N\ll N_0$. Notice that the synaptic coupling is asymmetric; that is, if $J_{\alpha\beta}\neq 0$, then $J_{\beta\alpha}=0$.

In Appendix A we show that the dynamics represented by the probability in Eq. (2) can be reduced to the Poisson (uncorrelated) dynamics for a subthreshold driving input in the following limits: (i) no synaptic coupling, $J\mapsto 0$; (ii) weak noise, $(\theta-c)/\eta\gg 1$; and (iii) long observation time, $M\tau\mapsto\infty$.

## III. FISHER INFORMATION

First we determine the Fisher information for a single neuron. This case is easier to analyze, and will enable us to obtain some insights into the more complicated case of many neurons. The latter case is analyzed subsequently.

### A. Single neuron

In order to calculate the Fisher information contained in a random signal $s(1),s(2),\ldots,s(M)$ given the parameter $x$, where $M$ is the number of time steps, one must determine the joint probability that a neuron at any time $k\tau\leqslant M\tau$ was at a certain state $s(k)$. The joint probability $P[s(1),s(2),\ldots,s(M);x]$ given input $x$, can be written in general as [39]

$$P[s(1),\ldots,s(M);x]=P[s(1);x]P[s(2)|s(1);x]\cdots \times P[s(M)|s(1),\ldots,s(M-1);x], \tag{5}$$

where $s(k)$ is defined as before. This equation is derived in Appendix B. The form of the conditional probability $P[s(k)|s(1),\ldots,s(k-1);x]$, that the neuron fires at time step $k$, indicates that it may depend on this neuron's past activity. In the present case, however, there is no history dependence and therefore that probability reduces to

$$P[s(k)|s(1),\ldots,s(k-1);x] \equiv P[s(k);x] = \frac{1}{2}\left(1+[2s(k)-1]\tanh\left[\frac{c(x)-\theta}{\eta}\right]\right). \tag{6}$$

Taking the above into account, one can rewrite Eq. (5) as

$$P[s(1),\ldots,s(M);x]=\prod_{i=1}^{M}P[s(i);x], \tag{7}$$

which greatly simplifies further analysis in determining the Fisher information. The Fisher information can be defined by [17]

$$I_F=-\sum_{s(1),\ldots,s(M)}P[s(1),\ldots,s(M);x] \times\frac{\partial^2\ln P[s(1),\ldots,s(M);x]}{\partial x^2}. \tag{8}$$

Substituting Eqs. (6) and (7) into Eq. (8) and performing the necessary algebra yields (cf. Appendix D),

$$I_F=\frac{M\tau}{\eta^2\cosh^2\dfrac{(c-\theta)}{\eta}}\left(\frac{\partial c}{\partial x}\right)^2. \tag{9}$$

The drive $c$ is a function of a stimulus $x$. In Sec. IV it is shown that the average firing rate is an increasing function of $c$. This implies that $c$ should depend on $x$ in a fashion qualitatively similar to the way the firing rate depends on $x$. It is experimentally well established [40] that the latter dependence, known as a tuning curve, often has a pronounced maximum. Guided by this, in this paper, we assume the following shape for the driving input of the neuron $\alpha$:

$$c_\alpha(x)=\begin{cases}\dfrac{A}{\sigma}(x-x_\alpha)+A, & x_\alpha-\sigma\leqslant x\leqslant x_\alpha\\ -\dfrac{A}{\sigma}(x-x_\alpha)+A, & x_\alpha\leqslant x\leqslant x_\alpha+\sigma\\ 0 \quad \text{otherwise,}\end{cases} \tag{10}$$

where $A$ is the amplitude of the stimulus-induced drive and is the same for every neuron (this amplitude is proportional to a contrast of a stimulus, and therefore we will call it also contrast interchangeably), $\sigma$ is a width of ''sensitivity'' of the drive $c_\alpha$ on a stimulus $x$ ($\sigma$ is the same for every neuron), and finally $x_\alpha$ is the value of a stimulus for which the drive is maximal. One can also view $\sigma$ as the parameter characterizing the size of a ''receptive field'' of each neuron.

Using the expression on the drive [Eq. (10)], one can rewrite Eq. (9). If we additionally average $I_F$ over different values $x_0$ of stimulus for which the drive is maximal $[x_0\mapsto x_\alpha$ in Eq. (10)], we obtain

$$\overline{I_F}=\frac{2AM\tau\rho_0}{\eta\sigma}\left[\tanh\left(\frac{A-\theta}{\eta}\right)+\tanh\left(\frac{\theta}{\eta}\right)\right], \tag{11}$$

where $\overline{I_F}=\int_{-1/2\rho_0}^{1/2\rho_0}dx_0\rho_0 I_F$, and averaging over $x_0$ is performed with a uniform distribution $\rho_0$. Such averaging may seem artificial in the case of a single neuron; however, for many neurons it is a necessity, since different neurons are, in general, exposed to different driving inputs.

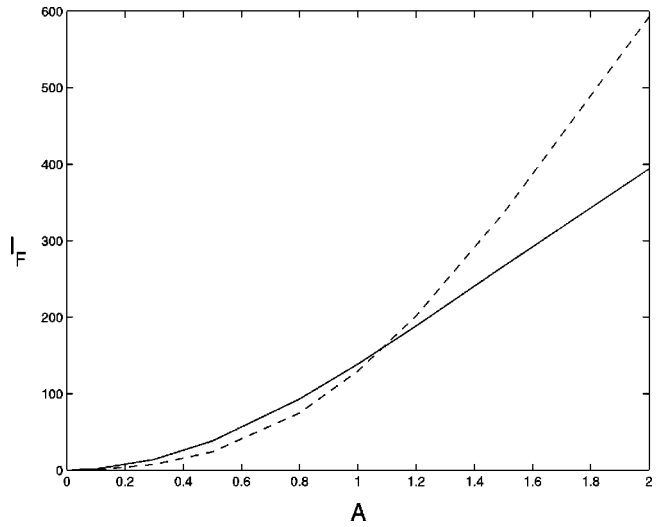


FIG. 1. Dependence of the Fisher information $\overline{I_F}$ on the amplitude $A$ (contrast) of the driving input without the short-term synaptic dynamics ($a=0$). Note that $\overline{I_F}$ is a monotonic, growing function of $A$. The solid line represents the excitatory network with $J=0.2$. The dashed line corresponds to the inhibitory network with $J=-0.2$. Other parameters are $M=100$, $\theta=\sigma=\tau=1.0$, $N_0=1000$, and $N=10$.

Formula (11) shows that, for a subthreshold driving input ($A<\theta$), the Fisher information takes a maximal value for a nonzero values of noise $\eta$. In the limits $\eta\mapsto 0$ and $\eta\mapsto\infty$, $\overline{I_F}$ vanishes. As we will see in Sec. III B, a similar conclusion will be valid for the case of many correlated neurons. Note that a scaling $\overline{I_F}\sim\sigma^{-1}$, proposed by Zhang and Sejnowski [8] in the firing rate type model, is also valid here; it will be valid in the case of many neurons as well. The latter dependence says that narrowly tuned stimulus-driven inputs are more advantageous in terms of information processing [4].

### B. Many neurons

The joint probability $P[\{s(1)\},\ldots,\{s(M)\};x]$ in the case of many coupled neurons can be written in general as [39]

$$P[\{s(1)\},\ldots,\{s(M)\};x] = \prod_{\alpha=1}^{N_0} P[s_\alpha(1);x]P[s_\alpha(2)|\{s(1)\};x]\cdots \times P[s_\alpha(M)|\{s(1)\},\ldots,\{s(M-1)\};x], \quad (12)$$

where $P[s_\alpha(k)|\{s(1)\},\ldots,\{s(k-1)\};x]$ is given by Eq. (2). The above form of the joint probability assumes that the activity of a given neuron at any given time depends on the past activities of all other neurons, and does not depend on those activities at that given time. In other words, we take into account some history-dependent correlations in the network. In our particular model, Eq. (12) can be further simplified by noting that, in fact, we have $P[s_\alpha(k)|\{s(1)\},\ldots,\{s(k-1)\};x]\equiv P[s_\alpha(k)|\{s(k-2)\},\{s(k-1)\};x]$, which is a consequence of the assumed form of the synaptic dynamics [compare Eqs. (2)–(4)]. To be more explicit, the state of each neuron in $k+1$ time step depends on the pattern of synaptic couplings in the $k$ time step, which in turn depends only on the state of the neurons in the $k-1$ time step. This means that every neuron can ''remember'' what happened in the network up to two time steps back. Derivation of Eq. (12) is presented in Appendix B.

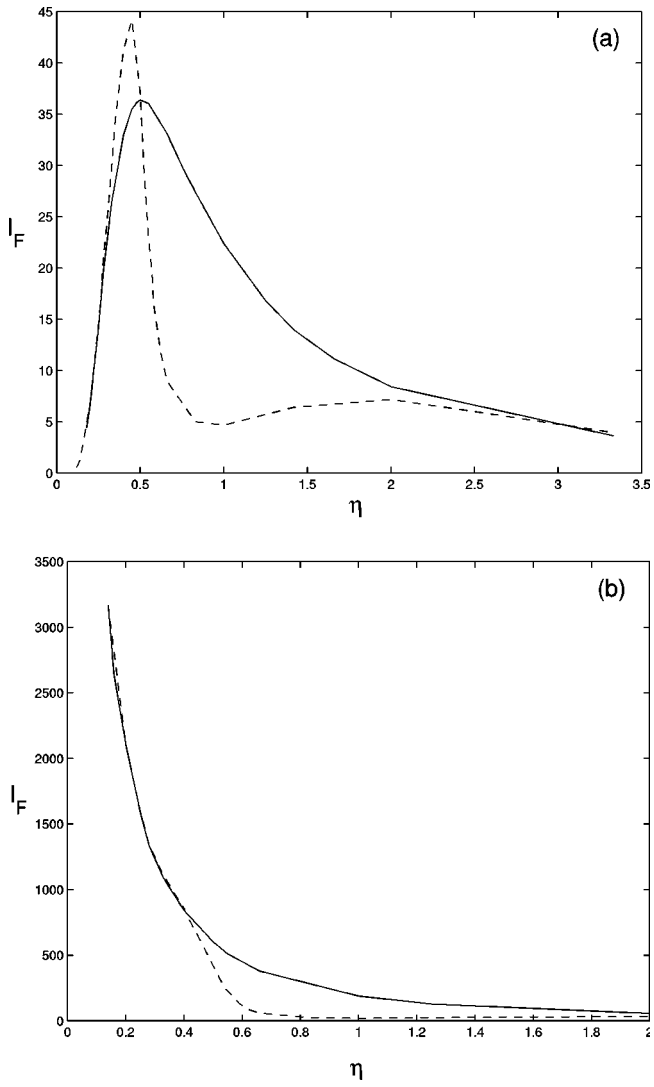


FIG. 2. Dependence of the Fisher information on the noise in the network. In both figures the solid line corresponds to an inhibitory network, and the dashed line to an excitatory network. (A) The case for the subthreshold driving input. Notice the pronounced maxima for some nonzero level of noise. An excitatory network exhibits additional smaller maximum. (B) The case for the suprathreshold driving input. Notice that $\overline{I_F}$ is maximal for noiseless networks and decays with an increasing level of noise. Parameters used: (A) $A=0.5$ and $J=0.3$ for the excitatory network, and $J=-0.3$ for the inhibitory network. (B) $A=1.2$, and the synaptic couplings are the same as in (A). Other parameters are exactly the same as in Fig. 1.

Having the joint probability, one can determine the Fisher information contained in the activities of the population of neurons in the network. As before, we average $I_F$ over a uniform distribution $\rho_0$ of all $\{x_\alpha\}$ for which drives are maximal. We obtain

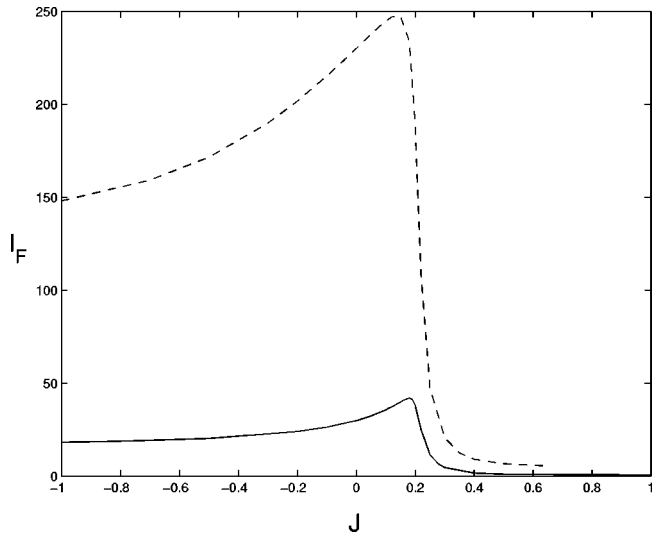


FIG. 3. Dependence of the Fisher information on the synaptic strength. The solid line corresponds to $A=0.5$ (subthreshold input), and the dashed line to $A=1.2$ (suprathreshold input). Note that the maxima of $\overline{I_F}$ fall to positive values of the synaptic couplings regardless of the magnitude of the driving inputs. Also note a steep decay of $\overline{I_F}$ for positive values of the synaptic couplings. The background noise value is $\eta=1$.

$$\overline{I_F}=\tau\sum_{i=1}^{M}\overline{I_F^{(i)}}, \tag{13}$$

where $\overline{I_F^{(i)}}$ is the averaged Fisher information per time at time step $i$. In Appendix C we sketch how to perform such averaging. In the limit $a\mapsto 0$, i.e., when the short-term synaptic plasticity is absent, and for low density $\rho_0$, $\overline{I_F^{(i)}}$ is given by

$$\begin{aligned}\overline{I_F^{(i)}}(a=0)=&\frac{AN_0\rho_0}{2^{N(i-1)-1}\eta\sigma}\sum_{k_1=0}^{N}\cdots\sum_{k_{i-1}=0}^{N}\\&\times F_1^{(i)}(\eta,J,\theta;k_1,\ldots,k_{i-1})\\&\times\left[\tanh\left(\frac{k_{i-1}J+A-\theta}{\eta}\right)\right.\\&\left.-\tanh\left(\frac{k_{i-1}J-\theta}{\eta}\right)\right]+O(\rho_0^2),\end{aligned} \tag{14}$$

with

$$\begin{aligned}&F_1^{(i)}(\eta,J,\theta;k_1,\ldots,k_{i-1})\\&\quad=\prod_{j=1}^{i-1}\binom{N}{k_j}\left[1+\tanh\left(\frac{k_{j-1}J-\theta}{\eta}\right)\right]^{k_j}\\&\qquad\times\left[1-\tanh\left(\frac{k_{j-1}J-\theta}{\eta}\right)\right]^{N-k_j},\end{aligned} \tag{15}$$

where integer $k_0=0$. Details of derivation of Eq. (14) are presented in Appendix D. The key assumption in deriving Eq. (14) is that the observation time $M\tau$ is not too long, so that one can neglect ''recurrent'' effects. From a technical point of view, this means that our expressions are valid as long as $M$ satisfies $NM<N_0$. This limit greatly simplifies the analysis, and computation of $I_F^{(k)}$ can be controlled at any time step $k$ satisfying $k<M$.

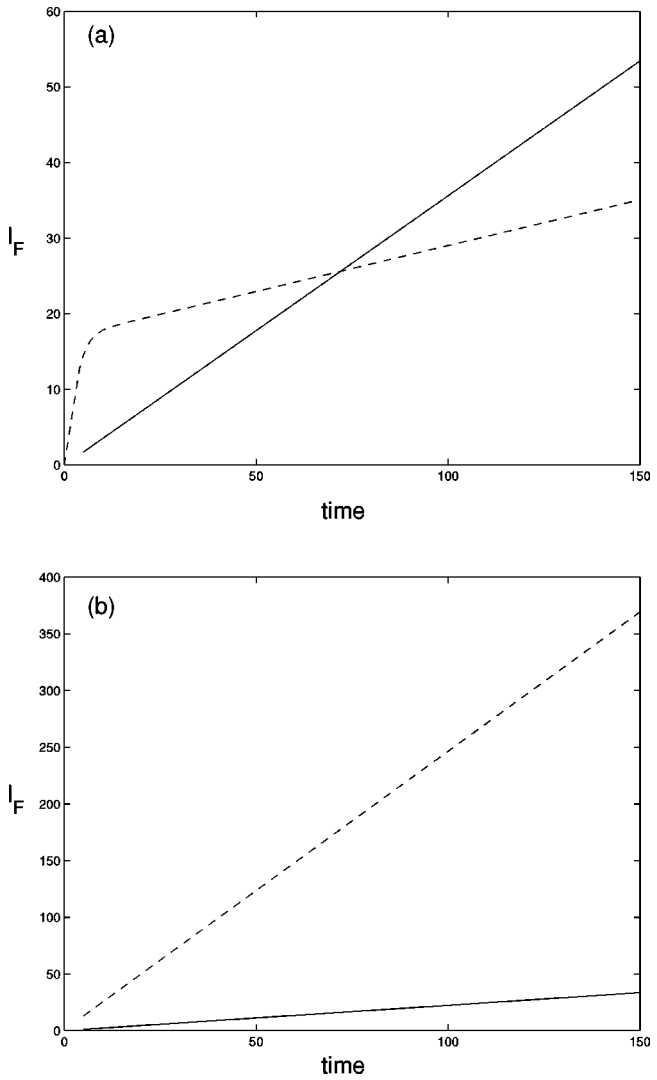


FIG. 4. Dependence of the Fisher information on the time course for excitatory (A) and inhibitory (B) networks. In both cases time is measured in units equal to $\tau$. (A) For not too strong synaptic couplings ($J=0.1$) and weak driving inputs ($A=0.5$), the dependence is almost linear (solid line). When the input and synapses become strong ($A=1.5$, $J=0.3$; dashed line) this dependence has two distinct regimes: fast initial growth and later a more slow growth. (B) Dependence of $\overline{I_F}$ on time for inhibitory networks is linear even for large driving inputs and strong synaptic coupling; the solid line corresponds to $A=0.5$ and $J=-0.3$, and the dashed line corresponds to $A=1.5$ and $J=-1.0$. Inhibitory networks, in general, provide more information about a stimulus (note the difference in scale).

The Fisher information grows linearly with the number of neurons $N_0$ in the network (keeping the number of connections $N$ per neuron constant). This suggests that the coding accuracy improves with increase of the size of the neuronal population. The same conclusion was reached in Ref. [6] for firing rate models. Also note that the Fisher information is optimal for narrowly tuned driving inputs (as before), because of the scaling $\overline{I_F}\sim\sigma^{-1}$.

The dependence of the Fisher information on the ampli-

tude of the drive, noise, synaptic strength, and time was determined numerically using Eqs. (14) and (15). An important finding, which will be used later, is that $\overline{I_F}$ grows with the amplitude $A$ of a drive (contrast), which means that the stronger the stimulus the better it is for coding. This dependence is depicted in Fig. 1.

Note that the dependence of $\overline{I_F}$ upon noise has a pronounced maximum for some finite $\eta$ if the driving input is subthreshold [Fig. 2(a)]. For a suprathreshold drive [Fig. 2(b)], the Fisher information has a maximum for $\eta=0$ and decreases monotonically with increasing noise. These behaviors are the same as in the case of a single neuron [see Eq. (11)]. In both cases, however, the noise ''window'' for which the network encodes stimulus optimally is narrow.

Dependence of the Fisher information on the synaptic strength (Fig. 3) reveals an interesting behavior. The peak of $\overline{I_F}$ falls to positive values of the synaptic coupling $J$, which shows that excitatory networks perform better in terms of the population coding. However, this is the case only in the vicinity of the maximum. For positive values of $J$ away from that maximum, $\overline{I_F}$ can be much smaller than for negative $J$. Thus excitatory networks are advantageous over inhibitory ones, but only in a limited range of values of the synaptic couplings.

Figure 4 shows that $\overline{I_F}$ is a growing function of the observation time $M\tau$. Again, we find a distinct behavior for excitatory and inhibitory networks. For excitatory networks [Fig. 4(a)], when the drive is subthreshold and the synaptic coupling not too strong, $\overline{I_F}$ depends almost linearly on time. However, when the drive is suprathreshold and coupling stronger, the growth of $\overline{I_F}$ has two phases: the initial phase is very fast, and $\overline{I_F}$ reaches substantial values quickly; and the second phase is much slower. For inhibitory networks [Fig. 4(b)], $\overline{I_F}$ grows almost linearly with time regardless of the magnitude of the drive and coupling.

Computation of the Fisher information when the short-term synaptic dynamics is included is more complicated. It can be made a little easier in the case of a network with very sparse connections for which $J_{\alpha\beta}=J\delta_{\alpha,\beta+1}$, i.e., when each neuron is connected only to one of the remaining neurons. For such a network one can find ($\rho_0\mapsto 0$)

$$\overline{I_F^{(i)}}(a)=\frac{AN_0\rho_0}{2^{2(i-2)}\eta\sigma}\sum_{m=0}^{1}\sum_{k_1=0}^{1}\cdots\sum_{k_{i-2}=0}^{1}\sum_{n_1=0}^{1}\cdots \times\sum_{n_{i-2}=0}^{1}H^{(i)}(\eta,J,a,\theta;\{k\},\{n\}) \times G^{(i)}(\eta,J,a,\theta;m,k_{i-2},n_{i-2},n_{i-3})+O(\rho_0^2), \tag{16}$$

where functions $G^{(i)}$ and $H^{(i)}$ are given by

$$G^{(i)}(\eta,J,a,\theta;m,k_{i-2},n_{i-2},n_{i-3}) =\left(1+\tanh\left[\frac{k_{i-2}J(1-an_{i-3})-\theta}{\eta}\right]\right)^{m} \times\left(1-\tanh\left[\frac{k_{i-2}J(1-an_{i-3})-\theta}{\eta}\right]\right)^{1-m} \times\left[\tanh\left(\frac{mJ[1-an_{i-2}]+A-\theta}{\eta}\right)-\tanh\left(\frac{mJ[1-an_{i-2}]-\theta}{\eta}\right)\right] \tag{17}$$

and

$$H^{(i)}(\eta,J,a,\theta;\{k\},\{n\})=\prod_{j=1}^{i-2}\left(1+\tanh\left[\frac{k_{j-1}J(1-an_{j-2})-\theta}{\eta}\right]\right)^{k_j}\left(1-\tanh\left[\frac{k_{j-1}J(1-an_{j-2})-\theta}{\eta}\right]\right)^{1-k_j} \times\left(1+\tanh\left[\frac{n_{j-1}J(1-ak_{j-2})-\theta}{\eta}\right]\right)^{n_j}\left(1-\tanh\left[\frac{n_{j-1}J(1-ak_{j-2})-\theta}{\eta}\right]\right)^{1-n_j}. \tag{18}$$

In the above expressions $k_{-1}=k_0=n_{-1}=n_0=0$. One can check that in the limit $a\mapsto 0$, Eq. (16) reduces to Eq. (14) with $N=1$ (for this see Appendix D). Notice that also here $\overline{I_F}\sim N_0$, indicating that larger populations of neurons are more accurate in coding.

As before, Eq. (16) has been solved numerically for different magnitudes of the synaptic plasticity $a$. The results are displayed in Fig. 5. For excitatory networks [Fig. 5(a)] there can be a substantial increase in the Fisher information by increasing the depression amplitude $a(a>0)$, provided the synaptic coupling is strong enough. For example, when $J=0.2$ ($A=0.5$), $\overline{I_F}$ stays almost constant regardless of $a$. However, when the coupling is increased, one can notice a dramatic increase in $\overline{I_F}$; for $J=2.3$ and threshold-equal driving input ($A=1.0$, $\theta=1.0$) there is 50% increase in $\overline{I_F}$ obtained by changing $a$ from zero to $a=0.8$; for $J=4.0$ and suprathreshold driving input ($A=1.2$, $\theta=1.0$), there is 500% increase in $\overline{I_F}$ [Fig. 5(a)]. Short-term synaptic facilitation ($a<0$) has the opposite effect on the Fisher information; it reduces $\overline{I_F}$, although not so dramatically. The surprising result is that for inhibitory networks the short-term synaptic plasticity does not have any significant influence on the Fisher information [Fig. 5(b)].

## IV. CORRELATION FUNCTIONS

It this section we study the relationship between temporal correlations among neurons and the accuracy of information processing. One would like to know whether temporal cor-

relations are advantageous or harmful for this task. In order to answer this question we calculate correlation functions and compare them with the Fisher information.

The correlation function $C_{\alpha\beta}$ between activities of the neurons $\alpha$ and $\beta$ is defined in a standard way,

$$C_{\alpha\beta}(k,j)=\langle s_\alpha(k+j)s_\beta(k)\rangle, \tag{19}$$

where symbol $\langle\cdots\rangle$ denotes averaging over noise, which formally means averaging with respect to the joint probability given by Eq. (12). This correlation function has the following interpretation. It is a measure of the probability that the neuron $\alpha$ fires at time step $k+j$, provided the neuron $\beta$ fired at time step $k$. Note that $C_{\alpha\beta}$ takes values only between 0 and 1, since $0\leqslant s_\alpha(k)\leqslant 1$.

The computed below correlation functions are nonstationary ones, since we do not assume that the network is in any equilibrium state (although such a state is reached after some initial time). Also, formulas below were derived for the case when the short-term synaptic dynamics is absent ($a\mapsto 0$). For delay correlation function, i.e., for $j\geqslant 1$, we obtain

$$\begin{aligned}\overline{\overline{C_{\alpha\beta}(k,j)}}=&\frac{1}{2^{N(k+j-1)+1}N}\sum_{n_1=0}^{N}\cdots\sum_{n_{k+j-1}=0}^{N}(N-n_k)\\&\times\left[1+\tanh\left(\frac{n_{k+j-1}J+c_\alpha-\theta}{\eta}\right)\right]\\&\times\left[1+\tanh\left(\frac{n_{k-1}J+c_\beta-\theta}{\eta}\right)\right]\\&\times F_1^{(k+j)}(\eta,J,\theta;n_1,\ldots,n_{k+j-1})+O(\rho_0),\end{aligned} \tag{20}$$

where the function $F_1^{(k+j)}$ was defined before in Eq. (15). For equal time correlation function, i.e., for $j=0$, we obtain

$$\begin{aligned}\overline{\overline{C_{\alpha\beta}(k,0)}}=&\frac{1}{2^{2N(k-1)+2}}\sum_{n_{\alpha,1}=0}^{N}\sum_{n_{\beta,1}=0}^{N}\cdots\sum_{n_{\alpha,k-1}=0}^{N}\sum_{n_{\beta,k-1}=0}^{N}F_2^{(k)}(\eta,J,\theta;\{n_\alpha\},\{n_\beta\})\left[1+\tanh\left(\frac{n_{\alpha,k-1}J+c_\alpha-\theta}{\eta}\right)\right]\\&\times\left[1+\tanh\left(\frac{n_{\beta,k-1}J+c_\beta-\theta}{\eta}\right)\right]+O(\rho_0),\end{aligned} \tag{21}$$

where

$$\begin{aligned}F_2^{(i)}(\eta,J,\theta;\{n_\alpha\},\{n_\beta\})=&\prod_{j=1}^{i-1}\binom{N}{n_{\alpha,j}}\binom{N}{n_{\beta,j}}\left[1+\tanh\left(\frac{(n_{\alpha,j-1}+n_{\beta,j-1})J-\theta}{\eta}\right)\right]^{n_{\alpha,j}+n_{\beta,j}}\\&\times\left[1-\tanh\left(\frac{(n_{\alpha,j-1}+n_{\beta,j-1})J-\theta}{\eta}\right)\right]^{2N-n_{\alpha,j}-n_{\beta,j}}.\end{aligned} \tag{22}$$

In Eqs. (20) and (21), symbol $\overline{\overline{C_{\alpha\beta}}}$ denotes averaging $C_{\alpha\beta}$ over all $\{x_\gamma\}$ except $x_\alpha$ and $x_\beta$. The equal time correlation function $\overline{\overline{C_{\alpha\beta}(k,0)}}$ is a measure of coincidence in the firing of the two neurons $\alpha$ and $\beta$. This fact makes it a suitable quantity for a comparison with the Fisher information, i.e., with the accuracy of the population coding. An interesting fact to note is that the correlation functions between the two neurons $\alpha$ and $\beta$ in Eqs. (20) and (21) are composed of the sum of the two products: factors with the driving inputs $c_\alpha$ and $c_\beta$, and factors with $F_1$ and $F_2$ functions. The former factors are directly related to a stimulus, whereas the latter are the network contributions. In the limit $J\mapsto 0$, i.e., without coupling, only the stimulus-dependent part remains; sums over the $F_1$ and $F_2$ functions yield a numerical factor [for this see Eq. (D14) in Appendix D].

The correlation functions [Eqs. (20) and (21)], are nonzero even when a stimulus is absent, i.e., when $c_\alpha=c_\beta=0$. We call these types of correlations stimulus-independent correlations. Their existence lies in the fact that there is some intrinsic noise $\eta$ in the network which causes some background spontaneous activity, i.e., neurons fire occasionally even without an external input. If the excitatory synaptic coupling between neurons is strong there can be quite large stimulus-independent correlations. For weak coupling ($J\mapsto 0$) and for the noiseless network ($\eta\mapsto 0$), stimulus-independent correlations are very weak. This can be seen formally by noting that factors $(1+\tanh[(nJ-\theta)/\eta])\mapsto 0$ when $\eta\mapsto 0$.

When a stimulus is present the drives are nonzero, since they reflect the appearance of a stimulus. The correlation functions are monotonic functions of the drives [see factors with tanh containing $c_\alpha$ and $c_\beta$ in Eqs. (20) and (21)], i.e., the larger the drives the stronger the correlations between neurons. The correlation is maximal when $c_\alpha$ and $c_\beta$ take their maximal values. This can happen only when $x_\alpha$ and $x_\beta$, the values of a stimulus for which driving inputs $c_\alpha$ and $c_\beta$ are maximal, are identical. That is, correlation is proportional to the degree of overlap between ''receptive fields'' $c_\alpha$ and $c_\beta$ of the two neurons. This type of correlation is termed a stimulus-driven correlation. It is important to note that one cannot, in general, decompose correlation functions into a sum of stimulus-independent and stimulus-dependent parts (this is possible only for very weak stimuli; then one can perform a Taylor-series expansion and drop higher order terms).

In Fig. 6, correlation function defined as $\overline{C_{\alpha\beta}}(j) \equiv (1/M)\Sigma_{k=1}^{M}\overline{C_{\alpha\beta}(k,j)}$ is plotted for different values of the synaptic coupling $J$. One can see a pronounced peak of $\overline{C_{\alpha\beta}}(j)$ for $j=0$ for excitatory networks, indicating a strong dependence between neurons. For inhibitory networks that peak is much smaller. The half-width of all peaks is approximately equal to $2\tau$, which is consistent with the degree of ''memory'' present in the network (cf. Sec. V).

In Fig. 7, peaks $\overline{C_{\alpha\beta}}(0)$ of the correlation function are plotted as a function of the amplitude $A$ of the driving inputs. This dependence is monotonic, similar to the dependence of $\overline{I_F}$ on $A$. These two facts indicate that the Fisher information $\overline{I_F}$ is proportional to the degree of correlations in a network, if those are stimulus-driven correlations. This result is one of the main results of this paper. Also note that correlations between two neurons are stronger when the locations of the maxima of their drives ($x_\alpha$ and $x_\beta$) are closer. That is, correlations increase with the degree of overlap of their receptive fields.

The relationship between correlations and noise displays an interesting feature (Fig. 8). For excitatory networks [Fig. 8(a)] correlations are optimal for some nonzero level of noise both for subthreshold and suprathreshold driving inputs. For inhibitory networks [Fig. 8(b)], correlations always grow with an increasing level of noise, initially quickly and later more slowly, regardless of the value of the drives. These results indicate that the probability of simultaneous firing for cells in an excitatory network is large for some intermediate noise, whereas for cells in inhibitory networks this probability grows with an increasing level of noise. This type of behavior is different from the dependence of the Fisher in-

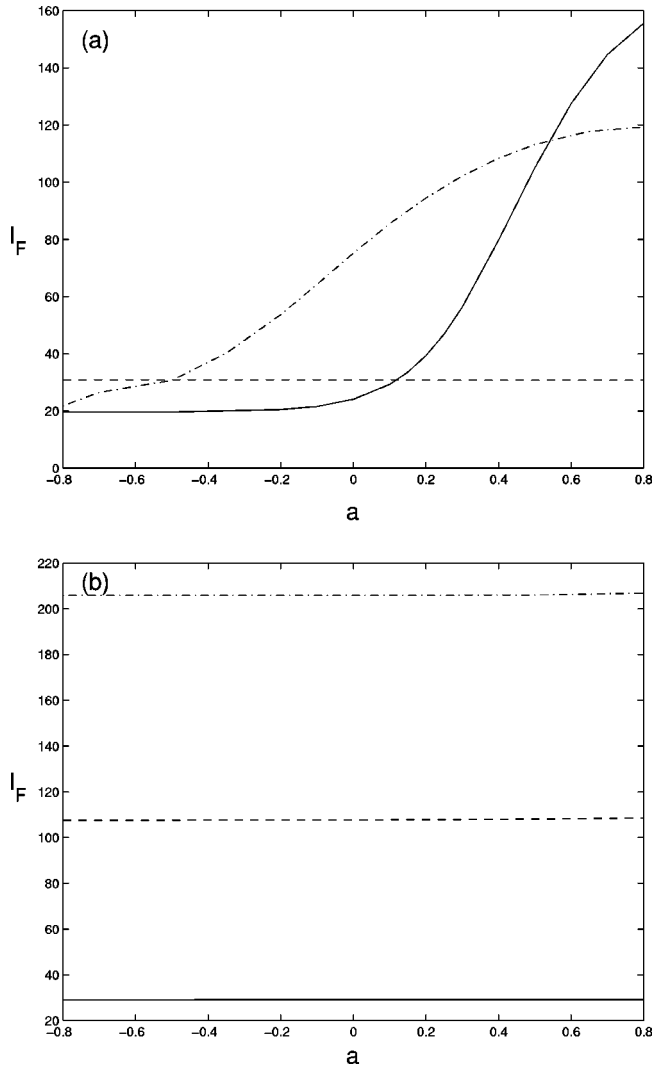


FIG. 5. Dependence of the Fisher information on the short-term synaptic plasticity parameter $a$ for excitatory (A) and inhibitory (B) networks. (A) The solid line corresponds to $J=4.0$ and $A=1.2$, the dash-dotted line to $J=2.3$ and $A=1.0$, and the dashed line to $J=0.2$ and $A=0.5$. Notice a dramatic increase in the Fisher information for strong stimuli and strong synaptic coupling. (B) The solid line corresponds to $J=-0.2$ and $A=0.5$, the dashed line to $J=-1.5$ and $A=0.9$, and the dash-dotted line to $J=-4.0$ and $A=1.2$. Notice that the Fisher information stays (almost) intact regardless of the amplitude of the short-term synaptic dynamics $a$. Background noise: $\eta=1$.

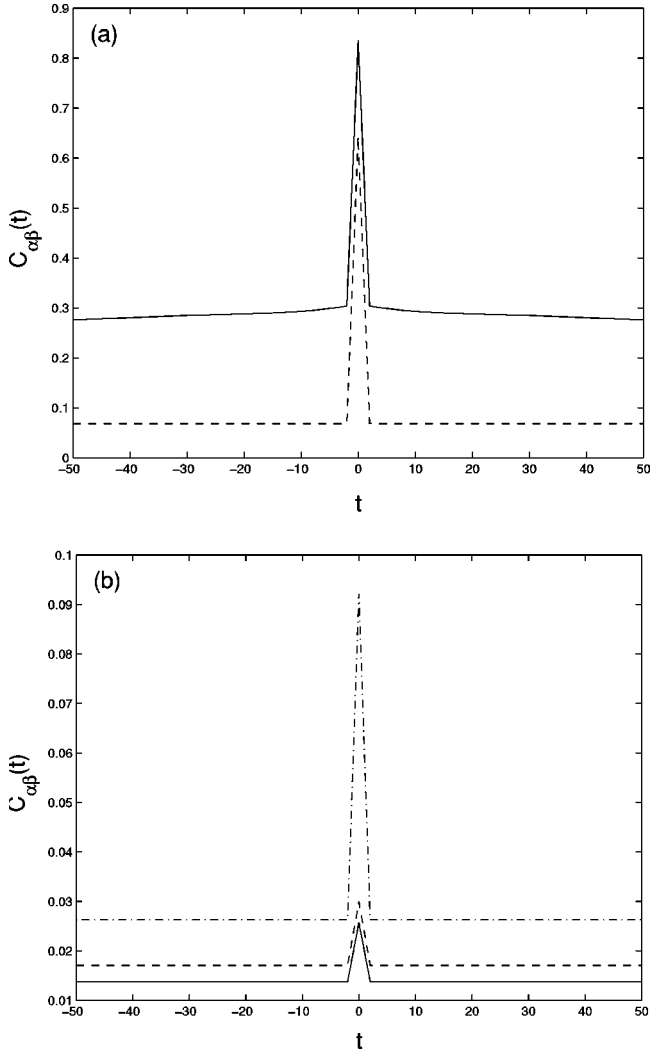


FIG. 6. Correlation function $\overline{C_{\alpha\beta}}(t)$ between two arbitrary neurons $\alpha$ and $\beta$ as a function of time $t$ (in $\tau$ units) for excitatory (A) and inhibitory (B) networks. (A) The solid line corresponds to $J=0.2$ and $A=0.5$, and the dashed line to $J=0.15$ and $A=0.5$. (B) The solid line corresponds to $J=-0.2$ and $A=0.5$, the dashed line to $J=-0.1$ and $A=0.5$, and the dash-dotted line to $J=-0.2$ and $A=1.2$. Note that neurons in the inhibitory networks are far less correlated.

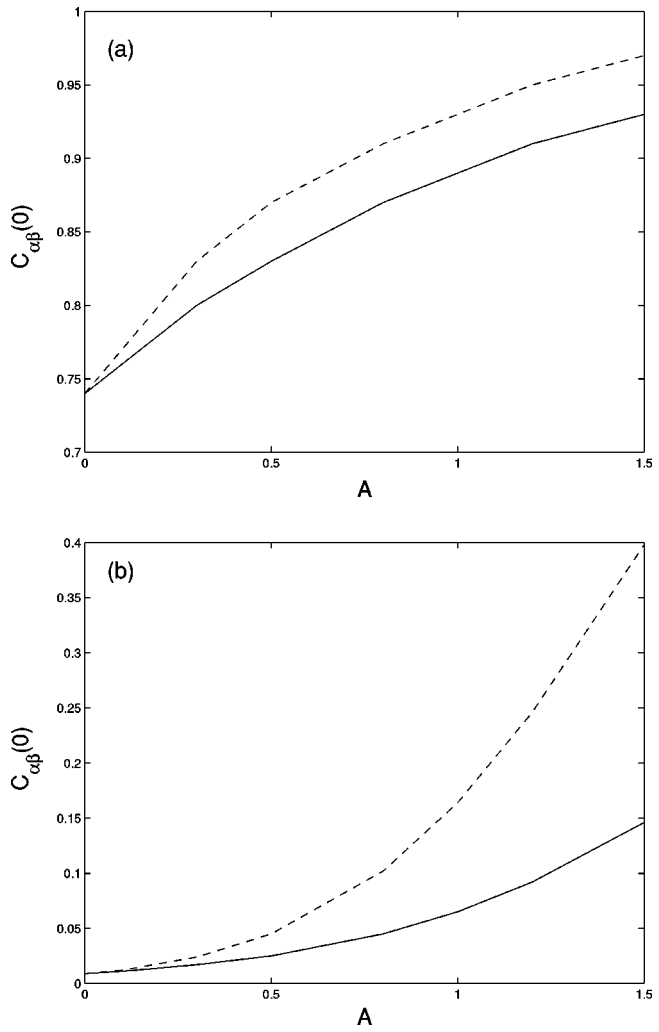


FIG. 7. The maxima of the correlation function $\overline{C_{\alpha\beta}}(0)$ as a function of the amplitude $A$ of the driving inputs. This dependence is monotonic, similarly as the dependence $\overline{I_F}$ upon $A$ (compare Fig. 1). (A) Excitatory networks: the solid line corresponds to $J=0.2$ with $x_\alpha - x_\beta = 0.8$, and the dashed line to $J=0.2$ with $x_\alpha - x_\beta = 0.1$. (B) Inhibitory networks: $J=-0.2$, $x_\alpha - x_\beta = 0.8$ (solid line), $J=-0.2$, $x_\alpha - x_\beta = 0.1$ (dashed line). The difference $x_\alpha - x_\beta$ is a measure of the degree of overlap between ''receptive fields'' of the two neurons $\alpha$ and $\beta$. The smaller this difference, the more they overlap ($\sigma = 1.0$). Notice that correlations are greater for neurons with more overlapped receptive fields.

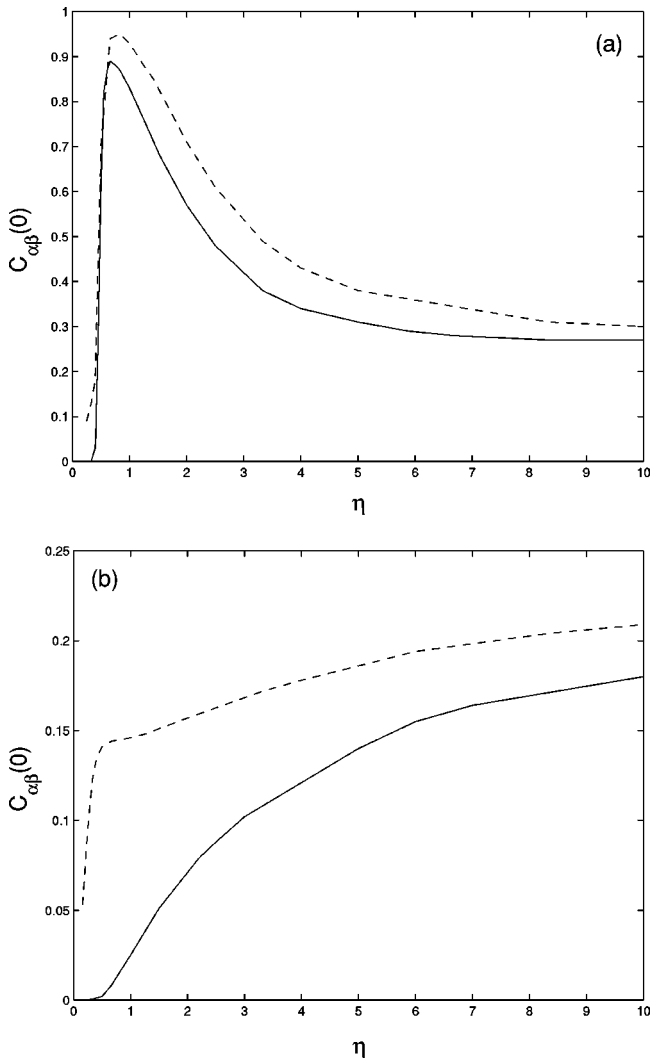


FIG. 8. Dependence of correlations upon noise in the network of excitatory (A) and inhibitory (B) neurons. For both networks this relationship is independent on the drive amplitude, i.e., subthreshold and suprathreshold inputs yield the same behavior. (A) Solid line: $J=0.2$ and $A=0.5$; dashed line: $J=0.2$ and $A=1.5$. Notice that correlations exhibit a pronounced maximum. (B) Solid line: $J=-0.2$ and $A=0.5$; dashed line: $J=-0.2$ and $A=1.5$. In this case correlations grow with an increasing level of noise. In both figures, $x_\alpha - x_\beta = 0.8$ and $\sigma = 1.0$.

formation on the noise (Fig. 2), suggesting that there is no explicit relation between $\overline{I_F}$ and the stimulus-independent correlations. This result is also one of the main results of this paper.

We also derived the average firing rate, which is proportional to $\langle s_\alpha(k)\rangle$. For very low density $\rho_0$ we obtain

$$\langle \overline{\overline{s_\alpha(k)}} \rangle = \frac{1}{2^{N(k-1)+1}} \sum_{n_1=0}^{N} \cdots \times \sum_{n_{k-1}=0}^{N} \left[ 1 + \tanh\left( \frac{n_{k-1}J + c_\alpha - \theta}{\eta} \right) \right] \times F_1^{(k)}(\eta, J, \theta; n_1, \ldots, n_{k-1}) + O(\rho_0), \quad (23)$$

where symbol $\overline{\overline{s_\alpha}}$ denotes averaging the quantity $s_\alpha$ with respect to all $\{x_\beta\}$ but $x_\alpha$. This expression shows that the average firing rate of the $\alpha$th neuron, which is equal to $\langle \overline{\overline{s_\alpha}} \rangle / \tau$, is a monotonic function of the driving input $c_\alpha$. Because of the noise, this neuron will fire occasionally even when the driving input is absent. Notice the network contribution through the presence of the $F_1$ functions. In the limit $J \mapsto 0$, i.e., when there is no coupling between neurons, the network contribution disappears and Eq. (23) reduces to

$$\langle \overline{\overline{s_\alpha}}(k) \rangle = \frac{1}{2}\left[ 1 + \tanh\left( \frac{c_\alpha(x) - \theta}{\eta} \right) \right], \quad (24)$$

which is a well known sigmoidal dependence of the firing rate on a driving input. Expressions (23) and (24) are consistent with an experimental fact from $V1$ of a cat that the

firing rate of a cell increases with contrast $A$ [40], which is proportinal to $c_\alpha$. In Appendix D we sketch how to obtain $\langle s_\alpha(k)\rangle$ and $\langle s_\alpha(k+j)s_\beta(k)\rangle$.

## V. DISCUSSION AND SUMMARY

The main result of this paper is in establishing a mutual relation between quasiprecise (see below) temporal correlations among neurons and the accuracy of the population coding. A quantitative measure of the accuracy of the population coding is provided by the Fisher information. This quantity was determined for both purely excitatory and purely inhibitory networks, in the limit of a not too long observation time when recurrent effects can be neglected, and compared with the maxima of the cross-correlation functions $\overline{C}_{\alpha\beta}(0)$ for two arbitrary neurons. If the change in the correlations between neurons is caused by a stimulus, then the Fisher information changes accordingly in a monotonic fashion. That is, if the amplitude of the drive increases then both the Fisher information (Fig. 1) and the temporal correlations (Fig. 7) grow. In Fig. 9 we display this one-to-one correspondence between the Fisher information and the stimulus-driven temporal correlations $\overline{C}_{\alpha\beta}(0)_{stim}$ between two arbitrary neurons $\alpha$ and $\beta$. This figure suggests that this type of correlation improves the coding accuracy. On the other hand, if the change in the correlations is caused by an intrinsic change in the network, such as the change in the level of noise, then there can be no monotonicity between such stimulus-independent correlations and the Fisher information. This can be seen by comparing the dependence of $\overline{I}_F$ and $\overline{C}_{\alpha\beta}(0)$ on the level of noise (Fig. 2 vs Fig. 8). Specifically, one can note that $\overline{C}_{\alpha\beta}(0)$ depends on the noise in the same fashion for both subthreshold and suprathreshold drives. This should be contrasted with the dependence of $\overline{I}_F$ upon noise, and the fact that subthreshold and suprathreshold signals yield different behaviors. In Fig. 10, we display the relationship between $\overline{I}_F$ and these stimulus-independent correlations $\overline{C}_{\alpha\beta}(0)_{noise}$. For subthreshold inputs, there is no monotonicity between these two quantities, and one can note many scattered points in Figs. 10(a) and 10(c). This pecular pattern is a consequence of the fact that in some intervals correlation is a double-valued function of the Fisher information. For suprathreshold inputs, stimulus-independent correlations are almost always harmful to the coding accuracy.

The above result that only stimulus-driven correlations always increase the accuracy of coding can be understood using the concept of mutual information. The mutual information $I_{mut}$ between activities of neurons and stimulus is a measure of their mutual dependency. Whenever the stimulus is changing, the output of the network changes accordingly and $I_{mut}$ provides a quantitative measure of this change. Since mutual information is directly related to the Fisher information in a monotonic way [5], this suggests that there should be a monotonic relationship between the stimulus and the Fisher information. This is why stimulus-driven correlations should improve the accuracy of population coding.

Our conclusion about the relationship between stimulus-driven correlations and the accuracy of coding is in agreement with experiment and analysis of Dan *et al.* [25]. Those authors studied the role of precise temporal correlations in a visual coding, and found that reconstruction of a stimulus is more accurate if these correlations are taken into account. They also found that temporal correlations between neurons are stronger for pairs of neurons with more greatly overlapping receptive fields. This is also consistent with our results (see Fig. 7).

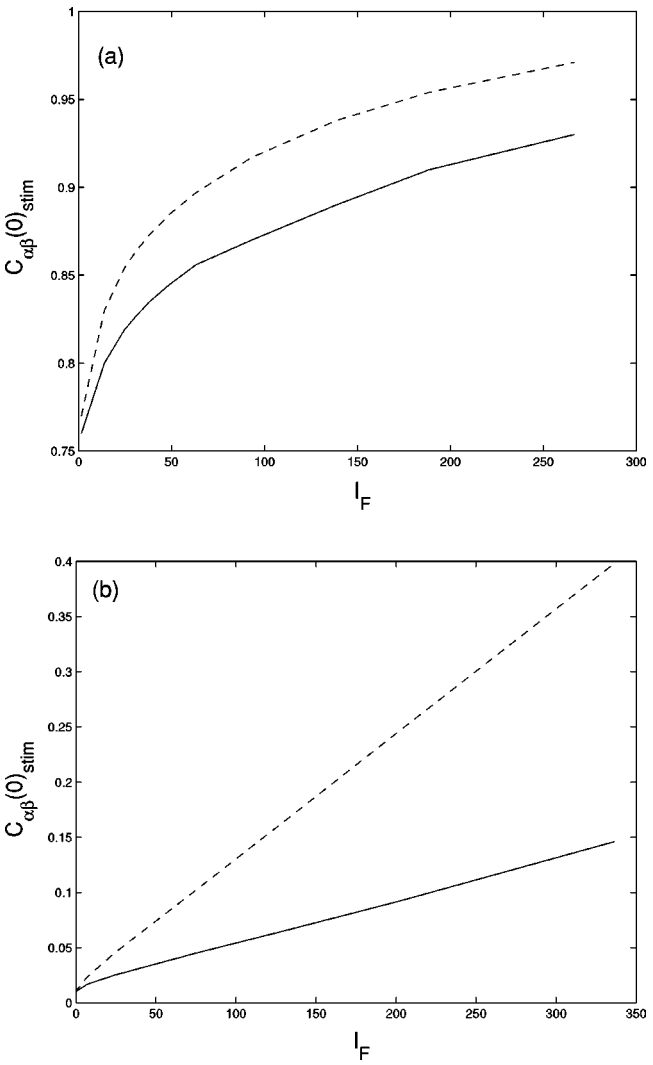


FIG. 9. The Fisher information vs stimulus-driven temporal correlations $\overline{C}_{\alpha\beta}(0)_{stim}$. We varied the amplitude $A$ of the driving input, and examined how the Fisher information and correlations were changing. (A) Excitatory network with $J=0.2$; the solid line corresponds to $x_\alpha - x_\beta = 0.8$, and the dashed line to $x_\alpha - x_\beta = 0.1$. (B) Inhibitory network with $J=-0.2$ and with the same graphical convention as in (A). Note that the Fisher information is a monotonic function of this type of correlation between neurons.

The precision of temporal correlations between neurons in the model studied in this paper is probably not too high. The length of the time bin $\tau$ is of the order of an effective membrane time constant, which is about 10–20 ms. For this reason, we are unable to say anything about correlations at smaller time scale 1–2 ms, relevant for a single spike width. Nevertheless, within this model one can still take into account the temporal pattern of spikes.

The level of intrinsic noise in the network also has an influence on the population coding. We found that this influ-

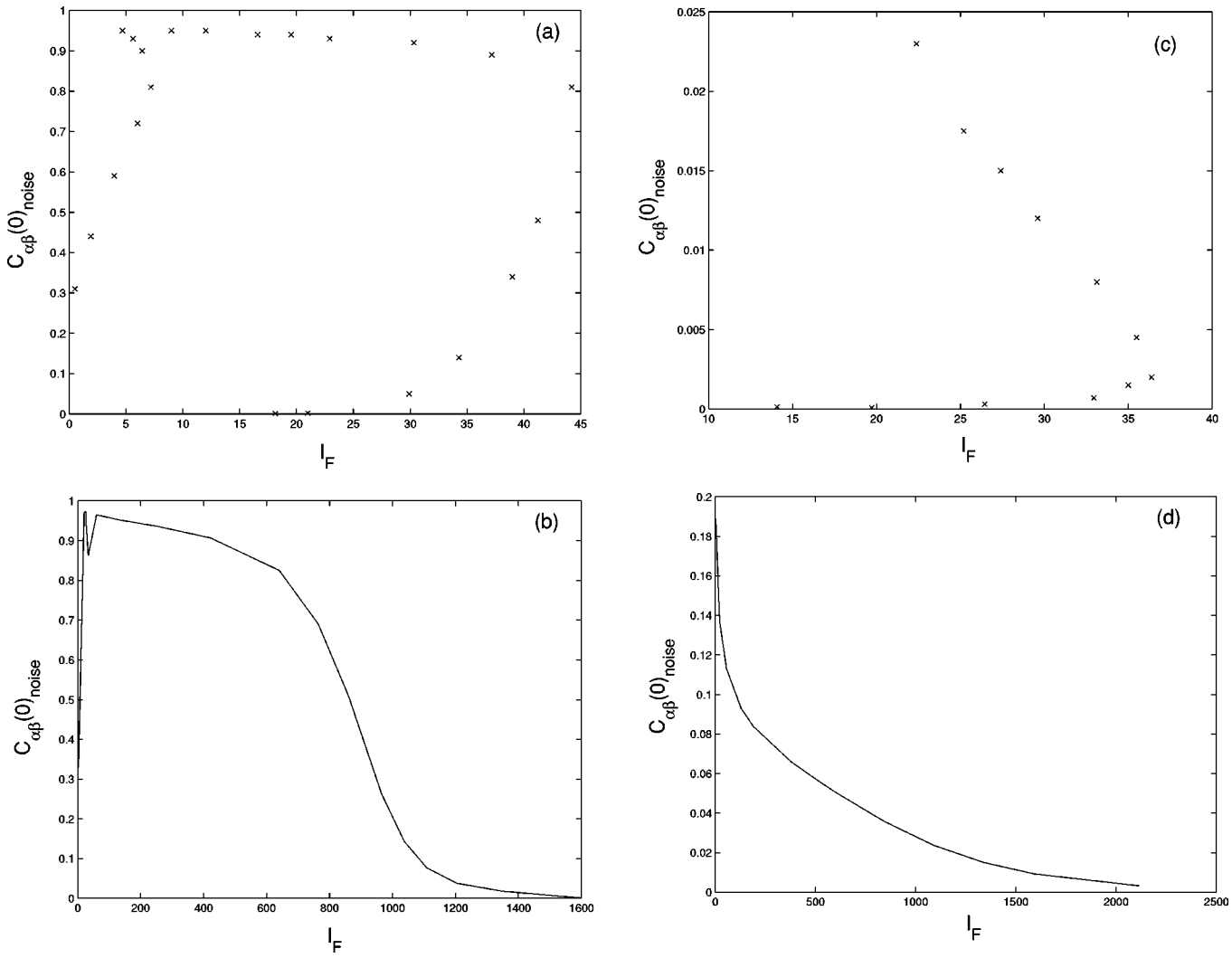


FIG. 10. The Fisher information vs stimulus-independent temporal correlations $\overline{C_{\alpha\beta}}(0)_{noise}$. We varied the level of noise, and examined how the Fisher information and correlations were changing. Cases (A) and (B) correspond to excitatory networks with $J=0.3$ and the driving inputs: subthreshold ($A=0.5$) (A), and suprathreshold ($A=1.2$) (B). Cases (C) and (D) correspond to inhibitory networks with $J=-0.3$ and the driving inputs: subthreshold ($A=0.5$) (C), and suprathreshold ($A=1.2$) (D). Notice that for subthreshold driving inputs there is no monotonicity between stimulus-independent correlations and the Fisher information [cases (A) and (C)]. For some intervals correlation $\overline{C_{\alpha\beta}}(0)_{noise}$ is a double-valued function of the Fisher information $I_F$. This is the reason why there are many scattered points in (A) and (C). For suprathreshold inputs noise-induced correlations almost always decrease the Fisher information [cases (B) and (D)].

ence depends strongly on the magnitude of the drive. If the amplitude of the drive is subthreshold, then the Fisher information has a maximum for some finite noise $\eta$ [Fig. 2(a)]. If the amplitude is suprathreshold then the Fisher information decreases with increasing noise [Fig. 2(b)], and is optimal when the noise is absent. In other words, the accuracy of coding is optimal for slightly noisy networks if the signal is subthreshold, and if the signal is suprathreshold the accuracy is optimal for noiseless networks. This behavior resembles the phenomenon of stochastic resonance [27–31], with the subtle difference that noise considered in this paper is an intrinsic property of the network, and not applied externally as in the standard stochastic resonance phenomenon. In the latter case there have been studies about the degree of coherence between the output and input of a system or information transfer, i.e., a mutual information, as a function of an external noise. The explanation for the noise-dependent behavior is as follows. When a signal is weak (subthreshold) then neurons fire very infrequently. The intrinsic noise can enhance the signal from time to time, such that the resulting signal crosses a threshold and there is an increase in the firing rate. This, in turn, increases the information transfer, since the latter is a monotonic function of the former for low firing rates [42,43]. For a higher level of noise, the signal is dominated by noise; therefore, it becomes more difficult to say something about the original signal. In the opposite regime, when the signal is strong (suprathreshold) then neurons fire very often. In such circumstances increasing the level of noise disrupts the signal, and hence decreases the information transfer (mutual information) and therefore reduces the Fisher information.

Note that the Fisher information can be much larger for suprathreshold stimuli [compare scales in Figs. 2(a) and 2(b)]. Also, it is apparent that purely inhibitory networks are

more broadly tuned to noise than purely excitatory networks. This feature might serve as one of the functional distinctions between these two types of networks.

Another example when inhibitory networks are more broadly tuned than excitatory ones is depicted in Fig. 3. One can see that the accuracy of the population coding is optimal for excitatory networks, but that inhibitory networks are more ''flexible'' because they are more broadly tuned. Excitatory networks perform optimally for a synaptic strength at about 0.15–0.2 of the value of the background noise.

The dependence of the Fisher information on the time course is presented in Fig. 4. The almost linear dependence of $\overline{I_F}$ on time can change into piecewise linear or nonlinear for sufficiently strong stimuli and for strong synaptic strength for excitatory networks. In that case, there can be a very rapid initial growth in $\overline{I_F}$ followed by a subsequent slower increase. This means that under certain conditions the processing of information about a stimulus can be very fast. There are experimental indications that a visual system processes information (face recognition) very quickly, at times of the order of hundreds of milliseconds or even faster [41,44–46], despite significant conduction delays caused by many recurrent cortical connections. This may suggest that the visual system uses basically a feedforward mechanism in early processing, with only a minor contribution coming from the recurrent connections [41]. However, we are unable to address this question explicitly within our approach, since the network architecture considered in this paper neglects recurrent connections, and this fact is clearly a limitation of the approach. Moreover, our network architecture is uniform with respect to the values of synaptic strength (it is either purely excitatory or purely inhibitory). Mixed networks could produce a more complex behavior.

The model for the short-term synaptic dynamics described by Eq. (4) neglects the resource (neurotransmitters) recovery. This process, which typically takes $\tau_{rec} \approx 100$ ms, can be incorporated into the model, in Eq. (4), by substituting sum $a\Sigma_{j=1}^{k-1} s_\beta(j)\exp[-(k-j)\tau/\tau_{rec}]$ for $a s_\beta(k-1)$, where $\tau$ is the time bin. Because the duration of the time bin is $\tau \sim 10$–$20$ ms, exponents with low $j$ decay rapidly and the major contribution to the sum yield the last few presynaptic spikes. The analysis in this paper is restricted only to the last presynaptic spike, i.e., the term $s_\beta(k-1)$. This term should capture the essence of the influence of the short-term synaptic dynamics on the accuracy of coding. The remaining terms in the sum would have an effect on the temporal correlations between neurons, leading to a broadening of peaks in the time-dependent correlation functions (Fig. 6). The characteristic width of those peaks, which characterizes the degree of memory in the network, would be of the order of $\tau_{rec}/\tau$.

The results of this work suggest that the short-term synaptic dynamics has an impact on the coding accuracy only for purely excitatory networks (Fig. 5). Depression and facilitation have opposite effects. That is, the former increases, and the latter decreases, the accuracy of coding. To gain an intuitive understanding of this behavior, note that depression, in general, reduces redundancy in a signal transmited between synaptically connected cells. On the other hand, facilitation enhances redundancy, because it amplifies the subsequent signals. Redundancy in a signal always decreases the information content [47]. Therefore, depression increases information transfer, whereas facilitation decreases it. Depressing synapses are especially optimal for very strong stimuli (suprathreshold) in networks with strong excitatory synaptic couplings [Fig. 5(a)]. This modulatory behavior of excitatory synapses may have important functional consequences for information processing in neural networks, e.g., in input layers of the cerebral cortex.

The fact that purely inhibitory networks are insensitive to short-term synaptic dynamics in terms of the population coding can be understood in the following way. By their nature, inhibitory synapses inhibit other cells from firing, reducing the information transfer between cells. For that reason, whether there is some process which modulates inhibitory synapses or not, it should not have any dramatic influence on the information transfer. Therefore, the accuracy of coding should stay unaffected. This conclusion is also consistent with Fig. 3.

Finally, the results of this paper confirm the previous finding [6] that the Fisher information is proportional to the number of neurons encoding information, regardless of the degree of correlations between them. This result suggests that larger networks should be more accurate (in principle) in decoding information about stimuli.

## ACKNOWLEDGMENTS

The author thanks Steve Epstein, Larry Abbott, and Nancy Kopell for useful comments on the manuscript. The work was supported by NSF Grant No. DMS 9706694.

## APPENDIX A

In this appendix we show how to reduce the dynamics of the model presented in this paper to the Poisson dynamics. Reduction to the Poisson uncorrelated dynamics is obtained when (i) there is no synaptic connections between neurons, i.e., in the limit $J \mapsto 0$; (ii) the noise is weak and the input is subthreshold, i.e., in the limits $(\theta - c)/\eta \gg 1$ and $c < \theta$; and (iii) the observation time $M\tau$ is large, i.e., in the limit $M \mapsto \infty$.

Probability that the neuron $\alpha$ is at state $s_\alpha(k)$ at time step $k$ is given by Eq. (2) in the text. When the condition (i) above is satisfied, this equation reduces to

$$P[s_\alpha(k)] = \frac{1}{2}\left[1 + (2s_\alpha(k) - 1)\tanh\left(\frac{c-\theta}{\eta}\right)\right]. \quad \text{(A1)}$$

Now including the second condition (ii) yields

$$\tanh\left(\frac{c-\theta}{\eta}\right) \approx -1 + 2e^{2(c-\theta)/\eta}. \quad \text{(A2)}$$

After insertion of this into Eq. (A1), one obtains the probability of firing $P[1]$ at any time step $k$ given by

$$P[1] \approx e^{2(c-\theta)/\eta}, \quad \text{(A3)}$$

and the probability of not firing $P[0]$ at any time step $k$ given by

$$P[0] \approx 1 - e^{2(c-\theta)/\eta}. \tag{A4}$$

The probability $P[n \text{ spikes}|M]$ of having $n$ spikes at time interval $M\tau$ is given by

$$\begin{aligned} P[n \text{ spikes}|M] &= \binom{M}{n} P[1]^n P[0]^{M-n} \\ &= \binom{M}{n} e^{2n(c-\theta)/\eta} [1 - e^{2(c-\theta)/\eta}]^{M-n}. \end{aligned} \tag{A5}$$

Next denoting $p \equiv e^{2(c-\theta)/\eta}$, and using the Stirling formula $k! \approx \sqrt{2\pi k}(k/e)^k$, which is valid for large natural $k$, we have

$$\begin{aligned} \lim_{M\to\infty} P[n \text{ spikes}|M] &= \lim_{M\to\infty} \frac{M^n}{n!} \sqrt{\frac{M}{M-n}} \left(\frac{M}{M-n}\right)^{M-n} \\ &\quad \times p^n (1-p)^{M-n} \\ &\approx \frac{M^n p^n}{n!} \lim_{M\to\infty} (1-p)^M. \end{aligned} \tag{A6}$$

The next step is to define a new quantity $q$ such that $Mp = q$. We keep this quantity constant, which means that $p$ must tend to zero. Including that, we obtain

$$\begin{aligned} P[n \text{ spikes}|M]_{M\mapsto\infty} &\approx \frac{(Mp)^n}{n!} \lim_{p\to 0} (1-p)^{q/p} \\ &= \frac{(Mp)^n}{n!} e^{-q} \\ &= \frac{(M \exp[2(c-\theta)/\eta])^n}{n!} \\ &\quad \times e^{-M \exp[2(c-\theta)/\eta]}. \end{aligned} \tag{A7}$$

The formula given by Eq. (A7) represents the standard Poisson process [39] with the mean firing rate equal to $\exp[2(c-\theta)/\eta]/\tau$.

## APPENDIX B

In this appendix we derive Eq. (12) in the main text. This equation is the joint probability for the activities of many neurons. However, it is instructive to start first with a single neuron case.

According to [39], the joint probability $P$ of a variable $s(t)$ at times $t_1 < t_2 < \cdots < t_M$ is given by

$$\begin{aligned} P(s_1, s_2, \ldots, s_M) &= P(s_1, \ldots, s_k) \\ &\quad \times P(s_{k+1}, \ldots, s_M | s_1, \ldots, s_k), \end{aligned} \tag{B1}$$

where $s_k = s(t_k)$ and $P(s_{k+1}, \ldots, s_M|s_1, \ldots, s_k)$ is a conditional probability that variable $s$ assumes values $s_{k+1}, \ldots, s_M$ at times $t_{k+1}, \ldots, t_M$, provided it had values $s_1, \ldots, s_k$ at previous times $t_1, \ldots, t_k$. From Eq. (B1), we easily obtain

$$\begin{aligned} P(s_1, s_2, \ldots, s_M) &= P(s_1, \ldots, s_{M-1}) P(s_M | s_1, \ldots, s_{M-1}) \\ &= P(s_1, \ldots, s_{M-2}) P(s_{M-1} | s_1, \ldots, s_{M-2}) P(s_M | s_1, \ldots, s_{M-1}) \\ &= \cdots = P(s_1) P(s_2|s_1) P(s_3|s_1, s_2) \cdots P(s_M | s_1, \ldots, s_{M-1}), \end{aligned} \tag{B2}$$

which is exactly Eq. (5) in the text.

Now let us find the joint probability for two neurons with correlated activity. If we denote an activity of the first neuron by $A$, and an activity of the second neuron by $B$, where $A = \{a_1, a_2, \ldots, a_M\}$ and $B = \{b_1, b_2, \ldots, b_M\}$, then from a formula $P(A,B) = P(A)P(B|A)$ and Eq. (B1), we obtain

$$\begin{aligned} P(a_1, b_1; a_2, b_2; \ldots; a_M, b_M) &= P(a_1, b_1; \ldots; a_{M-1}, b_{M-1}; a_M) P(b_M | a_1, b_1; \ldots; a_{M-1}, b_{M-1}; a_M) \\ &= P(a_1, b_1; \ldots; a_{M-1}, b_{M-1}) P(a_M | a_1, b_1; \ldots; a_{M-1}, b_{M-1}) \\ &\quad \times P(b_M | a_1, b_1; \ldots; a_{M-1}, b_{M-1}; a_M) \\ &= \cdots = P(a_1) P(b_1|a_1) P(a_2|a_1, b_1) P(b_2|a_1, b_1; a_2) \cdots P(a_M | a_1, b_1; \ldots; a_{M-1}, b_{M-1}) \\ &\quad \times P(b_M | a_1, b_1; \ldots; a_{M-1}, b_{M-1}; a_M). \end{aligned} \tag{B3}$$

In our network case we assume that the neuron $A$ at any time $t_k$ does not ''know'' anything about the activity of the neuron $B$ at that time. In other words, we assume that there is a certain small delay in information transfer. This assumption corresponds to the requirement that $b_k$ does not depend on $a_k$, and vice versa, so that

$$P(b_k|a_1,b_1;\ldots;a_{k-1},b_{k-1};a_k) \equiv P(b_k|a_1,b_1;\ldots;a_{k-1},b_{k-1}), \tag{B4}$$

which after insertion into Eq. (B3) gives

$$\begin{aligned} P(a_1,b_1;a_2,b_2;\ldots;a_M,b_M) &= P(a_1)P(b_1)P(a_2|a_1,b_1)P(b_2|a_1,b_1)\cdots \\ &\times P(a_M|a_1,b_1;\ldots;a_{M-1},b_{M-1}) \\ &\times P(b_M|a_1,b_1;\ldots;a_{M-1},b_{M-1}). \end{aligned} \tag{B5}$$

In the case of $N_0$ neurons one can easily generalize Eq. (B5) to

$$\begin{aligned} P[\{s(1)\},\{s(2)\},\ldots,\{s(M)\}] &= \prod_{\alpha=1}^{N_0} P[s_\alpha(1)]P[s_\alpha(2)|\{s(1)\}]\cdots \\ &\times P[s_\alpha(M)|\{s(1)\},\ldots,\{s(M-1)\}], \end{aligned} \tag{B6}$$

where $s_\alpha(k)$ is the activity of the $\alpha$th neuron at time $t_k$. This equation is exactly Eq. (12) in the text.

## APPENDIX C

In this appendix we show how to perform averaging over the distribution of the centers of the driving inputs $\{x_\alpha\}$. We assume that the maxima of the drives are independent on each other and are uniformly distributed with density $\rho_0$. Thus, for any quantity $Q[c_1(x),\ldots,c_{N_0}(x)]$, depending on the driving inputs $\{c_\alpha\}$ of all neurons, we have

$$\begin{aligned} \overline{Q}[\{c_\alpha\}] &= \int_{-1/2\rho_0}^{1/2\rho_0}\left(\prod_{i=1}^{N_0} dx_i\rho_0\right) Q[c_1(x),\ldots,c_{N_0}(x)] \\ &= \rho_0^{N_0}\int_{-1/2\rho_0}^{1/2\rho_0}\left(\prod_{i=2}^{N_0} dx_i\right)\left(\left(\int_{-1/2\rho_0}^{x-\sigma} dx_1+\int_{x+\sigma}^{1/2\rho_0} dx_1\right)\right. \\ &\times Q[0,c_2,c_3,\ldots,c_{N_0}]+\int_{x-\sigma}^{x} dx_1 \\ &\times Q\left[-\frac{A}{\sigma}(x-x_1)+A,c_2,\ldots,c_{N_0}\right] \\ &\left.+\int_x^{x+\sigma} dx_1 Q\left[\frac{A}{\sigma}(x-x_1)+A,c_2,\ldots,c_{N_0}\right]\right). \end{aligned} \tag{C1}$$

Performing the necessary algebra to the lowest order in density $\rho_0$ yields

$$\begin{aligned} \overline{Q}[\{c_\alpha\}] &= (1-2\rho_0\sigma)^{N_0}Q[0,0,\ldots,0] \\ &+2\rho_0(1-2\rho_0\sigma)^{N_0-1}\sum_{k=1}^{N_0}\int_0^\sigma d\zeta_k \\ &\times Q\left[0,\ldots,-\frac{A}{\sigma}\zeta_k+A,0,\ldots,0\right]+O(\rho_0^2). \end{aligned} \tag{C2}$$

The last equality can be further simplified for sparse density $\rho_0$, when $2\rho_0\sigma N_0 \ll 1$. In this limit we obtain

$$\begin{aligned} \overline{Q}[\{c_\alpha\}] &= Q[0,\ldots,0]+2\rho_0\sum_{k=1}^{N_0}\int_0^\sigma d\zeta_k Q\left[0,\ldots,0,\right. \\ &\left.-\frac{A}{\sigma}\zeta_k+A,0,\ldots,0\right]+O(\rho_0^2). \end{aligned} \tag{C3}$$

We will make use of this formula in Appendix D.

## APPENDIX D

In this appendix we sketch how to derive the Fisher information [Eqs. (14) and (16)], as well as the correlation functions [Eqs. (20) and (21)].

### 1. Derivation of the Fisher information

The first step is to rewrite the Fisher information [Eq. (8)], in a more convenient form,

$$\begin{aligned} I_F &= -\sum_{\{s\}} P[\{s\};x]\frac{\partial^2 \ln P[\{s\};x]}{\partial x^2} \\ &= \sum_{\{s\}}\frac{1}{P[\{s\};x]}\left(\frac{\partial P[\{s\};x]}{\partial x}\right)^2-\frac{\partial^2}{\partial x^2}\left(\sum_{\{s\}} P[\{s\};x]\right) \\ &= \sum_{\{s\}}\frac{1}{P[\{s\};x]}\left(\frac{\partial P[\{s\};x]}{\partial x}\right)^2, \end{aligned} \tag{D1}$$

since the joint probability $P[\{s\};x]$ is normalized, i.e., $\Sigma_{\{s\}}P[\{s\};x]=1$. Next, using the fact that the joint probability $P[\{s\};x]$ is represented by Eq. (12) in the text, we obtain

$$I_F(x)=\sum_{\{s\}}\sum_{i=1}^{M}\sum_{\beta=1}^{N_0}\frac{P[\{s\};x]}{P[s_\beta(i)|\{s(1)\},\ldots,\{s(i-1)\};x]^2}\left(\frac{\partial P[s_\beta(i)|\{s(1)\},\ldots,\{s(i-1)\};x]}{\partial x}\right)^2$$
$$+\sum_{\{s\}}\sum_{i,j=1}^{M}\sum_{\beta=1}^{N_0}\sum_{\gamma\neq\beta}^{N_0}\frac{P[\{s\};x]}{P[s_\beta(i)|\{s(1)\},\ldots,\{s(i-1)\};x]P[s_\gamma(j)|\{s(1)\},\ldots,\{s(j-1)\};x]}$$
$$\times\frac{\partial P[s_\beta(i)|\{s(1)\},\ldots,\{s(i-1)\};x]}{\partial x}\frac{\partial P[s_\gamma(j)|\{s(1)\},\ldots,\{s(j-1)\};x]}{\partial x}. \tag{D2}$$

The second term on the right hand side of the above equation vanishes. To see this, note that

$$\sum_{s_\beta(i)=0}^{1}\frac{\partial P[s_\beta(i)|\{s(1)\},\ldots,\{s(i-1)\};x]}{\partial x}$$
$$=\frac{1}{2}\sum_{s_\beta(i)=0}^{1}[2s_\beta(i)-1]\frac{\partial\tanh[R_\beta(i-1)/\eta]}{\partial x}=0. \tag{D3}$$

Thus one can write the Fisher information as

$$I_F(x)=\tau\sum_{k=1}^{M}I_F^{(k)}(x), \tag{D4}$$

where

$$I_F^{(k)}(x)=\sum_{\{s\}}\sum_{\alpha=1}^{N_0}\frac{P[\{s(1)\},\ldots,\{s(M)\};x]}{P[s_\alpha(k)|\{s(1)\},\ldots,\{s(k-1)\};x]^2}\times\left(\frac{\partial P[s_\alpha(k)|\{s(1)\},\ldots,\{s(k-1)\};x]}{\partial x}\right)^2. \tag{D5}$$

One can interpret $I_F^{(k)}$ as the Fisher information per time at $k$th time step.

#### *a. Single neuron*

Using Eqs. (D4) and (D5) one can derive Eq. (9) in the main text. In this case $N_0=1$, and the Fisher information at time step $k$ reads

$$I_F^{(k)}(x)=\sum_{\{s\}}\frac{\prod_{i=1}^{M}P[s(i);x]}{P[s(k);x]^2}\left(\frac{\partial P[s(k);x]}{\partial x}\right)^2$$
$$=\sum_{s(k)=0}^{1}\frac{1}{P[s(k);x]}\left(\frac{\partial P[s(k);x]}{\partial x}\right)^2, \tag{D6}$$

where we summed over all $\{s\}$ but $s(k)$ using the fact that $\Sigma_{s(l)=0}^{1}P[s(l);x]=1$ [see Eq. (D9) below]. Next steps are straightforward. Using Eq. (6), summing over $s(k)$, and using Eq. (D4), one obtains Eq. (9) in the text.

#### *b. Many neurons*

Since our $I_F$ depends on the driving inputs $\{c_\alpha\}$ of all neurons with different locations of maxima $\{x_\alpha\}$, one must average $I_F$ over those $\{x_\alpha\}$. In Appendix C we performed such averaging for any quantity $Q$ depending on $\{c_\alpha\}$. We can make use of Eq. (C3) from Appendix C and write

$$\overline{I_F}[A]=I_F[0,\ldots,0]+2\rho_0\sum_{k=1}^{N_0}\int_0^\sigma d\zeta_k I_F\left[0,\ldots,0,-\frac{A}{\sigma}\zeta_k+A,0,\ldots,0\right]+O(\rho_0^2). \tag{D7}$$

The first term on the right hand side of Eq. (D7) disappears. This is due to the fact that it does not depend on the driving inputs, or equivalently that $P[\{s(1)\},\ldots,\{s(M)\}]$ does not depend on $x$, and therefore a derivative with respect to $x$ in Eq. (D5) yields zero. Thus, to find $\overline{I_F}$ one must find $I_F(0,\ldots,0,c_\alpha,0,\ldots,0)$, which is present in the second term on the right hand side in Eq. (D7). Below we sketch how to do this.

### 2. Absence of the short-term synaptic dynamics

First, let us calculate $I_F^{(1)}$. According to Eq. (D5), we have

$$I_F^{(1)}=\sum_{\alpha=1}^{N_0}\sum_{\{s(1)\}=0}^{1}\cdots\sum_{\{s(M)\}=0}^{1}\frac{P[\{s(1)\},\ldots,\{s(M)\};x]}{P[s_\alpha(1);x]^2}\times\left(\frac{\partial P[s_\alpha(1);x]}{\partial x}\right)^2$$
$$=\sum_{\alpha=1}^{N_0}\sum_{\{s\}-s_\alpha(1)}\left(\prod_{\beta\neq\alpha}^{N_0}P[s_\beta(1);x]\right)\times\left(\prod_{\beta=1}^{N_0}P[s_\beta(2)|\{s(1)\};x]\cdots P[s_\beta(M)|\{s(1)\},\ldots,\{s(M-1)\};x]\right)\sum_{s_\alpha(1)=0}^{1}\frac{1}{P[s_\alpha(1);x]}\times\left(\frac{\partial P[s_\alpha(1);x]}{\partial x}\right)^2. \tag{D8}$$

The first summation after the second equality sign is performed over all $\{s(1)\},\ldots,\{s(M)\}$ except $s_\alpha(1)$. All these sums give 1, since

$$\sum_{s_\beta(k)=0}^{1} P[s_\beta(k)|\{s(1)\},\ldots,\{s(k-1)\};x]=\frac{1}{2}\sum_{s_\beta(k)=0}^{1}\left[1+(2s_\beta(k)-1)\tanh\left(\frac{R_\beta(k-1)}{\eta}\right)\right]=1. \tag{D9}$$

The remaining sum over $s_\alpha(1)$ is easy to perform:

$$\begin{aligned} I_F^{(1)} &= \sum_{\alpha=1}^{N_0}\sum_{s_\alpha(1)=0}^{1}\frac{[2s_\alpha(1)-1]}{[1+(2s_\alpha(1)-1)\tanh(R_\alpha(0)/\eta)]}\left(\frac{\partial\tanh(R_\alpha(0)/\eta)}{\partial x}\right)^2 \\ &= \sum_{\alpha=1}^{N_0}\cosh^2\left[\frac{R_\alpha(0)}{\eta}\right]\left(\frac{\partial\tanh[R_\alpha(0)/\eta]}{\partial x}\right)^2 \\ &= \sum_{\alpha=1}^{N_0}\frac{1}{\eta^2\cosh^2(R_\alpha(0)/\eta)}\left(\frac{\partial c_\alpha}{\partial x}\right)^2, \end{aligned} \tag{D10}$$

where $R_\alpha(0)=c_\alpha(x)-\theta$.

The term $I_F^{(2)}$ is calculated as follows

$$\begin{aligned} I_F^{(2)} &= \sum_{\alpha=1}^{N_0}\sum_{\{s\}}\frac{P[\{s(1)\},\ldots,\{s(M)\};x]}{P[s_\alpha(2)|\{s(1)\};x]^2}\left(\frac{\partial P[s_\alpha(2)|\{s(1)\};x]}{\partial x}\right)^2 \\ &= \sum_{\alpha=1}^{N_0}\sum_{\{s(1)\}}\sum_{s_\alpha(2)}\frac{1}{P[s_\alpha(2)|\{s(1)\};x]}\left(\frac{\partial P[s_\alpha(2)|\{s(1)\};x]}{\partial x}\right)^2\left(\prod_\beta P[s_\beta(1);x]\right)\sum_{\{s\}-\{s(1)\}-s_\alpha(2)}\left(\prod_{\beta\neq\alpha}P[s_\beta(2)|\{s(1)\};x]\right) \\ &\quad\times\left(\prod_{\beta=1}^{N_0}P[s_\beta(3)|\{s(1)\},\{s(2)\};x]\cdots P[s_\beta(M)|\{s(1)\},\ldots,\{s(M-1)\}]\right). \end{aligned} \tag{D11}$$

By the same argument as above, the summation over all $\{s\}$ different from $\{s(1)\}$ and $s_\alpha(2)$ yields 1. The summation over $s_\alpha(2)$ yields a similar result as before for $I_F^{(1)}$, with substitution $R_\alpha(1)$ for $R_\alpha(0)$. After that, one can write

$$\begin{aligned} I_F^{(2)} &= \sum_{\alpha=1}^{N_0}\sum_{s_1(1)=0}^{1}\cdots\sum_{s_\alpha(1)=0}^{1}\cdots\sum_{s_{N_0}(1)=0}^{1}\left(\prod_{\beta=1}^{N_0}P[s_\beta(1);x]\right)\frac{1}{\eta^2\cosh^2(R_\alpha(1)/\eta)}\left(\frac{\partial c_\alpha}{\partial x}\right)^2 \\ &= \sum_{s_{\alpha+1}(1)=0}^{1}\cdots\sum_{s_{\alpha+N}(1)=0}^{1}\left(\prod_{\beta=\alpha+1}^{\alpha+N}P[s_\beta(1);x]\right)\frac{1}{\eta^2\cosh^2(R_\alpha(1)/\eta)}\left(\frac{\partial c_\alpha}{\partial x}\right)^2 \\ &= \frac{1}{2^N\eta^2}\left(\frac{\partial c_\alpha}{\partial x}\right)^2\left(\frac{[1-\tanh(-\theta/\eta)]^N}{\cosh^2[(c_\alpha-\theta)/\eta]}+\binom{N}{1}\frac{[1-\tanh(-\theta/\eta)]^{N-1}[1+\tanh(-\theta/\eta)]}{\cosh^2[(J+c_\alpha-\theta)/\eta]}+\cdots\right. \\ &\quad\left.+\binom{N}{N}\frac{[1+\tanh(-\theta/\eta)]^N}{\cosh^2[(NJ+c_\alpha-\theta)/\eta]}\right). \end{aligned} \tag{D12}$$

Note that products in Eq. (D12) after the second equality contain $N$ terms. This reflects the fact that the $\alpha$th neuron is connected to $N$ other neurons denoted by $\alpha+1, \alpha+2, \ldots, \alpha+N$. The rest of terms $I_F^{(k)}$ are performed in the similar fashion. Term $I_F^{(3)}$ is equal to (as one can expect by analogy)

$$\begin{aligned} I_F^{(3)} &= \frac{1}{2^{2N}\eta^2}\sum_{\alpha=1}^{N_0}\left(\frac{\partial c_\alpha}{\partial x}\right)^2\sum_{k_1=0}^{N}\sum_{k_2=0}^{N}\binom{N}{k_1}\binom{N}{k_2}\frac{[1-\tanh(-\theta/\eta)]^{N-k_1}[1+\tanh(-\theta/\eta)]^{k_1}}{\cosh^2[(k_2J+c_\alpha-\theta)/\eta]}\left[1-\tanh\left(\frac{k_1J-\theta}{\eta}\right)\right]^{N-k_2}\left[1\right. \\ &\quad\left.+\tanh\left(\frac{k_1J-\theta}{\eta}\right)\right]^{k_2}. \end{aligned} \tag{D13}$$

The key assumption in deriving Eqs. (D10), (D12), and (D13) is $N\ll N_0$. As long as the observation time $M\tau$ is not too long, i.e., when $M$ satisfies the condition $NM<N_0$, the formulas for $I_F^{(k)}$ have the above relatively simple form. This is due to the fact that for such short times recurrent effects will not yet appear.

Next, using explicit form for the driving input $c_\alpha$ [Eq. (10)], we can perform integration of $I_F^{(k)}$ over $x$ according to Eq. (D7). Only terms with cosh depend on $x$. The result is Eq. (14) in the text.

In the limit $J \mapsto 0$, the Fisher information for many neurons given by Eqs. (13)–(15) reduces to $\overline{I_F}$ (multiplied by the number of neurons $N_0$) for a single neuron [Eq. (11)]. To see this, note that for $J \mapsto 0$ we have

$$\sum_{k_1=0}^{N} \cdots \sum_{k_{i-1}}^{N} F_1^{(i)}(\eta,\theta;J=0;k_1,\ldots,k_{i-1}) = \prod_{j=1}^{i-1} \sum_{k_j=0}^{N} \binom{N}{k_j} \left[1+\tanh\left(-\frac{\theta}{\eta}\right)\right]^{k_j} \left[1-\tanh\left(-\frac{\theta}{\eta}\right)\right]^{N-k_j} = \prod_{j=1}^{i-1} 2^N = 2^{N(i-1)}. \tag{D14}$$

### 3. Inclusion of the short-term synaptic dynamics

Slightly more complicated is calculation of $\overline{I_F}$ when short-term synaptic dynamics, i.e., when $a \neq 0$, is included. Repeating the same steps as before, one obtains Eq. (16) in the text. For the sake of consistency, we show below that Eq. (16) reduces to Eq. (14) in the limit $a \mapsto 0$. In this limit the $G^{(i)}$ function does not depend on $\{n\}$ indices, and we are able to sum over $\{n\}$. We have

$$\sum_{m=0}^{1} \sum_{k_1=0}^{1} \cdots \sum_{k_{i-2}=0}^{1} \sum_{n_1=0}^{1} \cdots \sum_{n_{i-2}=0}^{1} H^{(i)}(\eta,J,a=0,\theta;\{k\},\{n\}) G^{(i)}(\eta,J,a=0,\theta;m,k_{i-2}) = \sum_{m=0}^{1} \sum_{k_1=0}^{1} \cdots \sum_{k_{i-2}=0}^{1} G^{(i)}(\eta,J,a=0,\theta;m,k_{i-2}) \sum_{n_1=0}^{1} \cdots \sum_{n_{i-2}=0}^{1} H^{(i)}(\eta,J,a=0,\theta;\{k\},\{n\}). \tag{D15}$$

The sums over $\{n\}$ can be executed as follows:

$$\begin{aligned}\sum_{n_1=0}^{1} \cdots \sum_{n_{i-2}=0}^{1} H^{(i)}(\eta,J,a=0,\theta;\{k\},\{n\}) &= \left(\prod_{j=1}^{i-2} \left[1+\tanh\left(\frac{k_{j-1}J-\theta}{\eta}\right)\right]^{k_j} \left[1-\tanh\left(\frac{k_{j-1}J-\theta}{\eta}\right)\right]^{1-k_j}\right) \\ &\times \prod_{j=1}^{i-2} \left(\sum_{n_j=0}^{1} \left[1+\tanh\left(\frac{n_{j-1}J-\theta}{\eta}\right)\right]^{n_j} \left[1-\tanh\left(\frac{n_{j-1}J-\theta}{\eta}\right)\right]^{1-n_j}\right) \\ &= 2^{i-2} \prod_{j=1}^{i-2} \left[1+\tanh\left(\frac{k_{j-1}J-\theta}{\eta}\right)\right]^{k_j} \left[1-\tanh\left(\frac{k_{j-1}J-\theta}{\eta}\right)\right]^{1-k_j}.\end{aligned} \tag{D16}$$

If we now identify index $m$ with $k_{i-1}$ and insert the result of the summation into Eq. (16), we obtain Eq. (14) with $N=1$.

### 4. Derivation of the correlation functions

Analogically, one can determine $\langle s_\alpha(k)\rangle$ and $\langle s_\alpha(k+j)s_\beta(k)\rangle$. As an example, we show how to derive $\langle s_\alpha(k)\rangle$. According to a definition we have

$$\langle s_\alpha(k)\rangle = \sum_{\{s(1)\}} \cdots \sum_{\{s(k)\}} \cdots \sum_{\{s(M)\}} s_\alpha(k) P[\{s(1)\},\ldots,\{s(M)\};x]. \tag{D17}$$

Invoking the same argument as before [Eq. (D9)], we notice that all sums over $\{s(M)\},\ldots,\{s(k+1)\}$ yield 1. Thus the remaining sums read

$$\langle s_\alpha(k)\rangle = \sum_{\{s(1)\}} \cdots \sum_{\{s(k-1)\}} \left(\prod_{\beta=1}^{N_0} P[s_\beta(1);x] P[s_\beta(2)|\{s(1)\};x] \cdots P[s_\beta(k-1)|\{s(1)\},\ldots,\{s(k-2)\};x]\right) \times \frac{1}{2}\left[1+\tanh\left(\frac{\sum_\gamma \tilde{J}_{\alpha\gamma}(k-1)s_\gamma(k-1)+c_\alpha-\theta}{\eta}\right)\right]. \tag{D18}$$

Performing the first sum over $\{s(k-1)\}$ yields

$$\langle s_\alpha(k)\rangle = \sum_{\{s(1)\}} \cdots \sum_{\{s(k-2)\}} \left( \prod_{\beta=1}^{N_0} P[s_\beta(1);x] \cdots P[s_\beta(k-2)|\{s(1)\},\ldots,\{s(k-3)\};x] \right) \frac{1}{2^{N+1}}$$
$$\times \sum_{k=0}^{N} \binom{N}{k} \left[ 1+\tanh\left( \frac{\sum_\gamma \tilde{J}_{\alpha\gamma}(k-2)s_\gamma(k-2)-\theta}{\eta} \right) \right]^{N-k} \left[ 1-\tanh\left( \frac{\sum_\gamma \tilde{J}_{\alpha\gamma}(k-2)s_\gamma(k-2)-\theta}{\eta} \right) \right]^{k}$$
$$\times \left[ 1+\tanh\left( \frac{(N-k)J+c_\alpha-\theta}{\eta} \right) \right]. \tag{D19}$$

We see a similar pattern as before in deriving the Fisher information. Now, by analogy, it is not difficult to write the whole sum, and the result is Eq. (23) in the text. In a similar manner, one can determine $\langle s_\alpha(k+j)s_\beta(k)\rangle$.


[1] H. B. Barlow, T. P. Kaushal, and G. J. Mitchison, Neural Comput. **1**, 412 (1989).
[2] W. Bialek, F. Rieke, R. R. de Ruyter van Steveninck, and D. Warland, Science **252**, 1854 (1991).
[3] J. J. Atick, Network **3**, 213 (1992).
[4] H. S. Seung and H. Sompolinsky, Proc. Natl. Acad. Sci. USA **90**, 10 749 (1993).
[5] N. Brunel and J.-P. Nadal, Neural Comput. **10**, 1731 (1998).
[6] L. F. Abbott and P. Dayan, Neural Comput. **11**, 91 (1999).
[7] S. Panzeri, S. R. Schultz, A. Treves, and E. T. Rolls, Proc. R. Soc. London, Ser. B **266**, 1001 (1999).
[8] K. Zhang and T. J. Sejnowski, Neural Comput. **11**, 75 (1999).
[9] H. Yoon and H. Sompolinsky (unpublished).
[10] A. P. Georgopoulos, A. Schwartz, and R. E. Kettner, Science **233**, 1416 (1986).
[11] L. M. Optican and B. J. Richmond, J. Neurophysiol. **57**, 163 (1987).
[12] A. P. Georgopoulos, R. E. Kettner, and A. Schwartz, J. Neurosci. **8**, 2928 (1988).
[13] M. A. Wilson and B. McNaughton, Science **261**, 1055 (1993).
[14] E. Salinas and L. F. Abbott, J. Comput. Neurosci. **1**, 89 (1994).
[15] K. Zhang, I. Ginzburg, B. L. McNaughton, and T. J. Sej--nowski, J. Neurophysiol. **79**, 1017 (1998).
[16] M. W. Oram, P. Foldiak, D. I. Perrett, and F. Sengpiel, Trends Neurosci. **21**, 259 (1998).
[17] R. E. Blahut, *Principles and Practice of Information Theory* (Addison-Wesley, Reading, MA, 1988).
[18] A. Pouget, K. C. Zhang, S. Deneve, and P. E. Latham, Neural Comput. **10**, 373 (1998).
[19] T. J. Gawne and B. J. Richmond, J. Neurosci. **13**, 2758 (1993).
[20] E. Zohary, M. N. Shadlen, and W. T. Newsome, Nature (London) **370**, 140 (1994).
[21] E. Vaadia, I. Haalman, M. Abeles, H. Bergman, Y. Prut, H. Slovin, and A. Aertsen, Nature (London) **373**, 515 (1995).
[22] R. C. deCharms and M. M. Merzenich, Nature (London) **381**, 610 (1996).
[23] A. Riehle, S. Grun, M. Diesmann, and A. M. H. J. Aertsen, Science **278**, 1950 (1997).
[24] D. Lee, N. L. Port, W. Kruse, and A. P. Georgopoulos, J. Neurosci. **18**, 1161 (1998).
[25] Y. Dan, J. M. Alonso, W. M. Usrey, and R. C. Reid, Nature Neurosci. **1**, 501 (1998).
[26] H. P. Snippe and J. J. Koenderink, Biol. Cybern. **67**, 183 (1992).
[27] J. K. Douglass, L. Wilkens, E. Pantazelou, and F. Moss, Nature (London) **365**, 337 (1993).
[28] S. M. Bezrukov and I. Vodyanoy, Nature (London) **378**, 362 (1995).
[29] J. J. Collins, T. T. Imhoff, and P. Grigg, J. Neurophysiol. **76**, 642 (1996).
[30] J. E. Levin and J. P. Miller, Nature (London) **380**, 165 (1996).
[31] S. F. Traynelis and F. Jaramillo, Trends Neurosci. **21**, 137 (1998).
[32] J. J. Hopfield, Proc. Natl. Acad. Sci. USA **79**, 2554 (1982).
[33] D. J. Amit, H. Gutfreund, and H. Sompolinsky, Phys. Rev. A **32**, 1007 (1985).
[34] P. Peretto, Biol. Cybern. **50**, 51 (1984).
[35] A. V. M. Herz, Z. Li, and J. L. van Hemmen, Phys. Rev. Lett. **66**, 1370 (1991).
[36] I. Ginzburg and H. Sompolinsky, Phys. Rev. E **50**, 3171 (1994).
[37] H. Markram and M. Tsodyks, Nature (London) **382**, 807 (1996).
[38] L. F. Abbott, K. Sen, J. A. Varela, and S. B. Nelson, Science **275**, 220 (1997).
[39] N. G. van Kampen, *Stochastic Processes in Physics and Chemistry* (North-Holland, Amsterdam, 1981).
[40] G. Sclar and R. Freeman, Exp. Brain Res. **46**, 457 (1982).
[41] M. W. Oram and D. I. Perrett, J. Neurophysiol. **68**, 70 (1992).
[42] R. Stein, Biophys. J. **7**, 797 (1967).
[43] F. Rieke, D. Warland, R. de Ruyter van Steveninck, and W. Bialek, *Spikes: Exploring the Neural Code* (MIT Press, Cambridge, MA, 1997).
[44] M. J. Tovee, E. T. Rolls, A. Treves, and R. P. Bellis, J. Neurophysiol. **70**, 640 (1993).
[45] E. T. Rolls and M. J. Tovee, Proc. R. Soc. London **257**, 9 (1994).
[46] S. Thorpe, D. Fize, and C. Marlot, Nature (London) **381**, 520 (1996).
[47] C. E. Shannon and W. Weaver, *The Mathematical Theory of Communication* (University of Illinois Press, Urbana, IL, 1949).